Spatial and temporal variability of lake accumulation rates in Subarctic Northwest Territories, Canada

by

Carley Angela Crann

A thesis submitted to the Faculty of Graduate and Postdoctoral Affairs in partial fulfillment of the requirements for the degree of

Master of Science

in

Earth Sciences

Carleton University
Ottawa, Ontario

Abstract

We examined the spatial and temporal variability of Holocene lake sediment accumulation at 22 sites from 18 lakes transecting boreal forest, tree line, and tundra zones in the central Northwest Territories, Canada. Over 140 radiocarbon dates were obtained, and accumulation rates (AR) were calculated at 100-year intervals from age-depth models constructed using the age-depth modeling software Clam. Sites with the shortest mean AR of 25±10yr/cm (1σ) occur primarily in the boreal zone. Sites with moderate (70±22yr/cm) and long (160±56yr/cm) AR are north of the treeline and display higher variability, strongly influenced by bathymetry. Many age-depth models are characterized by fluctuations in ARs that coincide with paleogeographical changes associated with proglacial lake evolution during the early Holocene, and subsequent climate changes inferred from proxy data. The insights gained on the spatial and temporal trends in ARs across the region are valuable for developing higher resolution age-depth models using the Bayesian software Bacon.

Acknowledgements

I would like to express deep gratitude to my supervisor Dr. R. Timothy Patterson. Tim has been very supportive throughout this project and I appreciate the opportunities he has given me. His enthusiastic attitude toward the Tibbitt to Contwoyto Winter Road (TCWR) project and his sense of humor are what kept spirits high among the lab group (the PRG) over these past few years. The PRG is a special bunch and we've had a great time working together, learning, debating, and talking science. I would like to specially acknowledge the efforts of Andrew Macumber (soon to be Dr. Macumber), who taught me the ropes in the lab and who has been a mentor to me over the past few years.

In the spring of 2012 I was fortunate to spend three months at Queen's University in Belfast taking courses and absorbing knowledge from Dr. Paula Reimer and Dr. Maarten Blaauw – world experts in radiocarbon dating and age-depth modeling. I was also lucky to work with Dr. Helen Roe, who is one of the most caring and dedicated advisors I have ever met.

Funding for this collaborative research project was provided by a NSERC Strategic Project Grant and Discovery Grant awarded to Dr. Patterson. Direct and in-kind funding was provided by the Northwest Territories Geoscience Office, Polar Continental Shelf Project, The Department of Aboriginal Affairs and Northern Development Canada (by, in part, a Cumulative Impacts and Monitoring Program award to Jennifer M. Galloway), the Geological Survey of Canada, the Tibbitt to Contwoyto Winter Road Joint Venture (Erik Madsen and the crew of the Dome, Lockhart, and Lac de Gras maintenance camps), EBA Engineering Consultants Ltd., the North Slave Métis Alliance, IMG Golder, Inuvik, and Golder Associates, Yellowknife.

I would like to thank my parents, siblings and in-laws for their unconditional love and support and for never letting me forget that family comes first. To my close friends, thank you for keeping me sane with coffee/beer dates and lots of UNTZ. Finally, I would like to thank my best friend and husband Jay for keeping me fuelled with delicious curries, motivating me everyday to keep on track, and for always making sure I am smiling.

Table of Contents

List of Tables

List of Figures

List of Appendices

1. Introduction

Age-depth models are essential in paleolimnological studies, as they provide a time-scale for past events and make it possible to correlate multiple studies across a region. Often built predominantly on radiocarbon dates from a limited number of dated horizons in a core, age-depth models are constructed to estimate the calendar ages for depths between those dated horizons. Assumptions as to how the deposit accumulated are inherent in these models. Over the past decade, significant advances have been made in age-depth modeling techniques, namely the integration of multimodal probability distributions of calibrated radiocarbon dates using numerical simulations (Blaauw and Heegaard, 2012), and the integration of prior knowledge for a site using Bayesian statistics (Christen, 1994; Buck et al., 1996; Buck and Millard, 2004). Robust knowledge of priors is particularly important for sections of an age-depth model where the behavior of the model is uncertain (e.g. sparse data, age reversals, age offsets, dates within a radiocarbon plateau). Priors differ based on how the information is deduced and how it is incorporated into the model. For example, the stratigraphic ordering of dates inherent in the data is built into Bayesian software, whereas marker horizons such as a tephra and pollen, or hiatuses and slumps are determined empirically and incorporated as discrete events. The final category of priors has to be estimated based on knowledge on how similar deposits have accumulated over time. This information is fed to the software as model parameters. Specifically, the Bayesian software Bacon requires an estimate of deposition time in years/cm (Blaauw and Christen, 2011).

Goring et al. (2012) provided a summary of deposition times from 152 lacustrine sites in the northeastern US region and found that, in general, lakes in the northeast US

region accumulated at rates of around 20 yr/cm, which is fairly similar to the previous findings of Webb and Webb (1988; 10 yr/cm) for the same region. However, these deposition times are far too rapid for the Subarctic and Arctic lakes examined here, where a short ice-free season and the lack of extensive terrestrial plant debris lead to slow accumulation rates. Thus, information of deposition times of lakes in northern Canada are required to produce the most accurate age-depth models using advances modeling techniques.

Accumulation rate data is also critical to the reconstruction of certain proxy data such as past fire events and rates of vegetation change (Koff et al., 2000; Marlon et al., 2006). The rate of sediment accumulation is not constant and can be affected by climate change. For example, in the Cathedral Mountains of British Columbia, an increase in sedimentation rate correlates with the development of a colder climate that reduced vegetation cover and led to increased erosion and sediment deposition (Evans and Slaymaker, 2004). Similarly, in a crater lake in equatorial East Africa, Blaauw et al. (2011) found that cooler climate conditions were associated with reduced vegetation, and increased terrestrial erosion. By using paired dating of bulk sediment and macrofossils, Blaauw et al. (2011) demonstrated that variations in an old-carbon offset was caused by a variable contribution of old terrestrial organic matter eroded from soils within the crater basin.

The research presented here work is part of a collaborative project aimed at better understanding the impact of climate change on the long-term viability of the strategically important Tibbitt to Contwoyto Winter Road (TCWR) in the Northwest Territories, Canada. In the central Canadian Subarctic, millennial-scale patterns of climatic change

during the Holocene have been identified from proxy evidence in sediment records (Moser and MacDonald 1990; MacDonald et al. 1993; Wolfe et al. 1996; Pienitz et al. 1999; Huang et al. 2004; Rühland and Smol 2005; MacDonald et al. 2009; Paul et al. 2010), but with higher sampling resolution of proxy data and more precise age-depth models, it may be possible to elucidate climate patterns at a much higher resolution (Galloway et al., 2010; Macumber et al., 2012). Paleoclimate patterns that operate on decadal time scales are of great interest to the land-use planners, natural resource managers, and developers responsible for Canada's billion-dollar mineral industry located largely in the remote regions of Northwest Territories accessible only by the winter road. In this research we expand upon the temperate lake research of Goring et al. (2012) and Web and Web (1988) by presenting accumulation rate data from 14 new sites and 8 sites previously studied in Subarctic Northwest Territories, Canada. We summarize Holocene accumulation rates for the 22 lacustrine sites based on classical age-depth models constructed using the software Clam (Blaauw, 2010). Because this is a much smaller dataset than Webb and Webb (1988) and Goring et al. (2012), we are able to take a closer look at the intricacies of each model (e.g. outliers, freshwater reservoir effect) and discuss the spatial and temporal variation in accumulation rates. As was suggested by Goring et al. (2012), regional datasets such as this can serve as a strong base of prior knowledge to inform Bayesian (and other) age models.

2. Regional setting

Lakes investigated in this study are located in the central Northwest Territories (Fig. 2.1) in an area underlain by a stable piece of the Canadian Shield known as the Slave Craton. Because bedrock geology plays a major role in lake and basin dynamics, we used the margin of the Slave Craton to constrain the study area for purposes of incorporating previous work. This section of Archean crust is characterized by a depositional and volcanic history that has been overprinted by multiple phases of deformation and intruded by granitoid plutons (Bleeker, 2002). Major rock units include basement gneisses and metavolcanics, metasedimentary rocks (turbidites), and widespread gneissic–granitoid plutons (Padgham and Fyson, 1992; Helmstaedt, 2009). The bedrock geology lacks carbon rich rocks such as limestones or marls, and is not likely to be a source of '^{14}C dead' carbon, which could cause radiocarbon dates to appear anomalously old.

The rolling terrain exhibits a gentle relief of only a few tens of meters, shaped by the glacial-erosional processes that prevailed during the last glacial maximum (Rampton, 2000). Where bedrock is not exposed, it lies beneath deposits of till and glaciofluvial sediment of varying thickness. The action of glacial erosion and subglacial meltwater flow has resulted in a landscape with abundant, often interconnected lakes. Regional deglaciation occurred in a northeastward direction around 10,000–9000 years BP (Dyke and Prest, 1987; Dyke et al., 2003). Figure 2.1 shows the approximate western margin of the Laurentide Ice Sheet as it retreated toward to east, sometime between 10,500 and 9900 years BP (Dyke and Prest, 1987) as well as the maximum extent of proglacial Lake McConnell (Smith, 1994). Lake McConnell was the main proglacial lake in the region following the retreat of the Laurentide Ice Sheet.

The present-day treeline runs NW/SE across the study area, roughly reflecting the polar front (Fig. 2.1; Huang et al., 2004). The treeline is marked by the northern limits of the boreal forest (Fig. 2.2a) where forest stands are open and lichen woodlands merge into areas of shrub tundra (Galloway et al., 2010; Fig. 2.2b). Soils are poorly developed with discontinuous permafrost south of the treeline, and continuous north of the treeline (Clayton et al., 1977). Tundra vegetation is composed of lichens, mosses, sedges, grasses, and diverse herbs (MacDonald et al., 2009). It is often affected by polygonal permafrost features (Fig. 2.2c), and is discontinuous on rocky substrates. Appendix A shows summer photos from each lake.

The climate of the region is subarctic continental, characterized by short summers and long cold winters. Annual precipitation is low (175 – 200 mm) and mean daily January temperatures range from -17.5°C to -27.5°C, while mean daily July temperatures range from 7.5°C to 17.5°C (Galloway et al., 2010). Lakes in the region are often ice-covered for much of the year, with an average open-water period of only 90 days (Wedel et al., 1990).

Broad-scale patterns of Holocene climate change in the study area have been identified by proxy evidence in lake sediment cores from Toronto Lake (MacDonald et al., 1993; Wolfe et al., 1996; Pienitz et al., 1999), Waterloo Lake (MacDonald et al., 1993), Lake S41 (MacDonald et al., 2009), Queen's Lake (Moser and MacDonald, 1990; MacDonald et al., 1993; Wolfe et al., 1996; Pienitz et al., 1999), McMaster Lake (Moser and MacDonald 1990; MacDonald et al., 1993), UCLA Lake (Huang et al., 2004), Slipper Lake (Rühland and Smol, 2005), and Lake TK-2 (Paul et al., 2010) (Fig. 2.1; Table 2.1). Many of these studies infer three main stages of landscape development: (1)

the first stage occurred between delgaciation (~9000 yr BP) and about 6000 yr BP when erosion decreased greatly in response to vegetation development from tundra to *Betula* dominated shrub tundra, and finally to spruce forest tundra (UCLA lake; Huang et al., 2004); (2) the second stage spanned from about 6000 to 3500 yr BP and was marked by a period of rapid forest-tundra expansion to about 50 km north of treeline (Queen's and Toronto lakes; Moser and MacDonald, 1990; MacDonald et al., 1993), likely reflecting a northward retreat of the polar front following the demise of the ice sheet in the middle Holocene (Huang et al., 2004); and (3) during the third stage from 3000 yr BP to the present, cooling climate occurred. This resulted in degradation of vegetation to the modern *Betula*-dominated shrub tundra of more northern sites (UCLA lake; Huang et al., 2004).

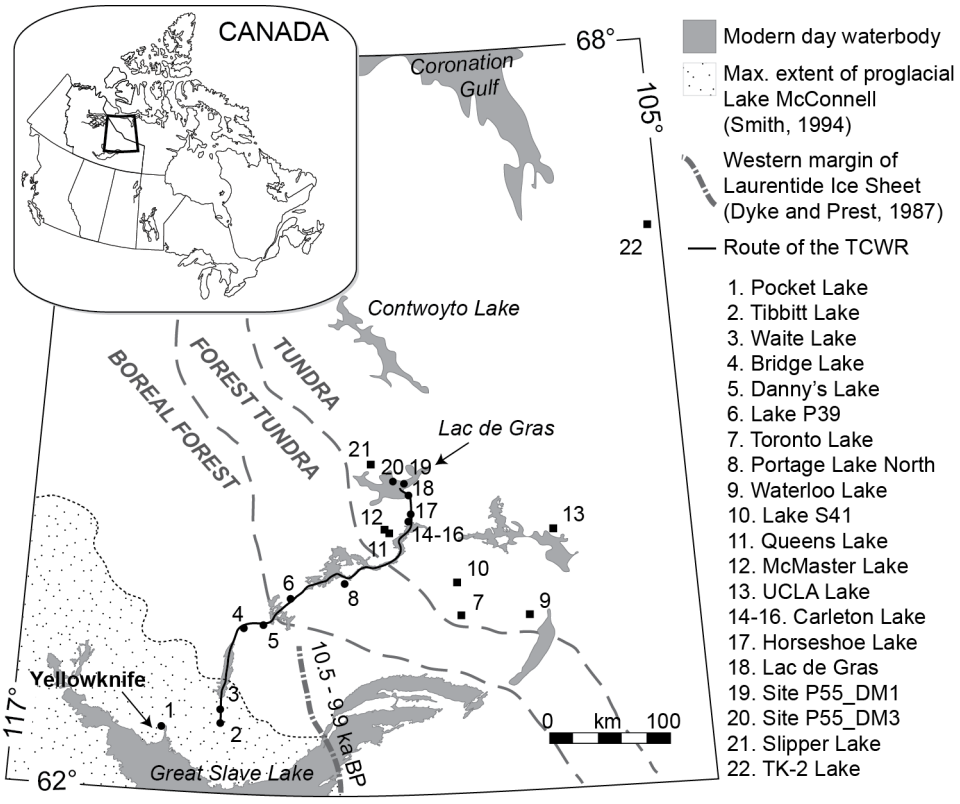

Figure 2.1 Map of the Northwest Territories showing the locations of core sites. Circles are sites from the TCWR project, squares are sites from previously published work, dashed lines show current boundaries between tundra, forest tundra, and boreal forest ecozones, and the inset shows the location of the study area within Canada.

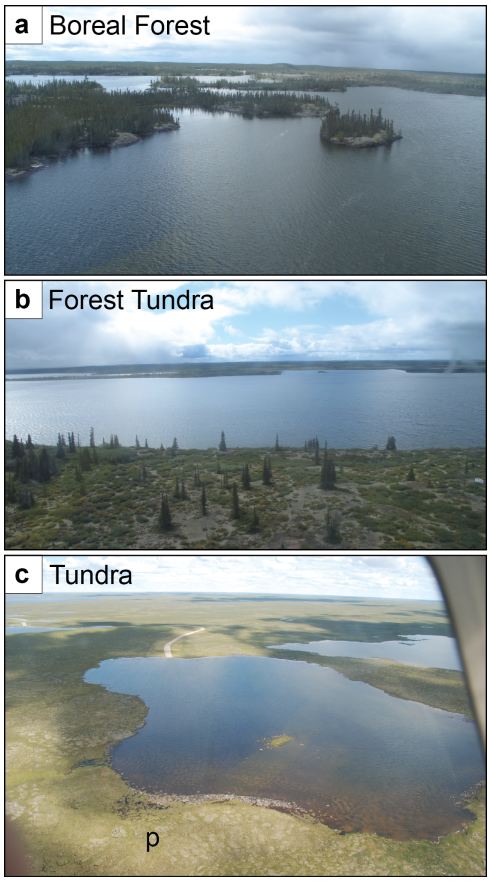

Figure 2.2 (a) Boreal forest zone at Waite Lake, (b) forest tundra zone near Portage Lake North (Mackay Lake, not mentioned in this paper), and (c) tundra zone at Carleton Lake, where "p" shows an area with polygonal soil. At Carleton Lake, the path of the TCWR can be seen exiting the lake to the north.

Table 2.1 Coordinates and physical characteristics of the lakes used in this study. For lakes not starting with P#, the core depth is often the maximum depth in the lake.

Site ID	Site name	Latitude	Longitude	Surface area (ha)	Water depth (cm)	inlets/ outlets	Citation
1	Pocket Lake (2FR, F1)	62°30.540	114°22.314	6	350	no	
2	P0 (Tibbitt)	62°32.800	113°21.530	300	672	yes	10, 11
3	P14-2 (Waite)	62°50.987	113°19.643	100	180	yes	10, 11
4	P26 (Bridge)	63°23.297	112°51.768	119.5	450	no	11
5	P34 (Danny's)	63°28.547	112°32.250	4.4	440	no	11
6	P39	63°35.105	112°18.436	37.3	110	no	11
7	Toronto	63°25.800	109°12.600	10	675	yes	2, 4, 5
8	P47 (Portage N.)	63°44.538	111°12.957	194.9	485	yes	11
9	Waterloo	63°26.400	108°03.600	?	?	minor	2
10	S41	63°43.110	109°19.070	<0.3	440	yes	8
11	Queens	64°07.000	110°34.000	50	450	no	1–5
12	McMaster	64°08.000	110°35.000	12	800?	minor	1, 2
13	UCLA	64°09.000	107°49.000	28	770	?	6
14	P49-1A	64°15.571	110°05.878	29.8	150	no	11
15	P49-1B	64°15.571	110°05.878	29.8	150	no	11, 12
16	R12_P49	64°15.500	110°05.928	29.8	300	no	
17	P52 (Horseshoe)	64°17.381	110°03.701	505	400	yes	11
18	P55 (Lac de Gras)	64°25.794	110°08.168	~57 k	400	yes	11
19	P55_DM1 (LdG)	64°30.393	110°15.255	~57 k		yes	
20	P55_DM3 (LdG)	64°33.723	110°26.841	~57 k		yes	
21	Slipper	64°37.000	110°50.000	190	1400	yes	7
22	TK-2	66°20.900	104°56.750	2.8	750?	yes	9

Citations: (1) Moser and MacDonald, 1990; (2) MacDonald et al., 1993; (3) Edwards et al., 1996; (4) Wolfe et al., 1996; (5) Penitz et al., 1999; (6) Huang et al., 2004; (7) Rühland and Smol, 2005; (8) MacDonald et al., 2009; (9) Paul et al., 2010; (10) Galloway et al., 2010; (11) Macumber et al., 2012; (12) Upiter et al., *in press?*

3. Methods

3.1 Core collection

Fourteen cores were obtained from ten lakes using a freeze core (Galloway et al., 2010; Macumber et al., 2012). Two lakes had up to three cores taken from them to assess inter-lake variability. Cores were not, or were unlikely to have been, obtained from the maximum depth of each lake. Bathymetry data is lacking for many of the lakes, so Zmax was unknown. We were also logistically restricted to coring locations where snow was cleared from the ice surface. These locations were exclusively along the route of the Tibbitt to Contwoyto Winter Road, which runs across the centre of lakes it traverses in most cases so that wave action generated by road traffic does hit the bottom of the lake (and reflect to disturb the ice the road is built upon).

The coordinates of each lake as well as basic lake parameters (surface area, core depth, inlets/outlets) for each site, along with the appropriate references are summarized in Table 2.1. The locations of the coring stations used for each lake are shown in figure 3.1, along with rough bathymetric contours when the data was available. Bathymetric data was obtained from EBA Engineering Consultants Ltd. All data was collected during a through-ice bathymetric survey using a ground penetrating radar (GPR) system towed behind a vehicle. Real time positioning was achieved using a survey grade GPS unit.

Cores from the TCWR project were collected using freeze corers, which are hollow, metal-faced corers filled with dry ice (Galloway et al., 2010; Macumber et al., 2012; see Appendix A for photos). Freeze corers are ideal for the extraction of cores in unconsolidated and water-saturated sediment as they capture sediment by in situ freezing (Lotter et al., 1997; Glew et al., 2001; Kulbe and Niederreiter, 2003; Blass et al., 2007).

In 2009, Tibbitt and Waite lakes were cored using a single faced freeze corer (Galloway et al., 2010). The Waite Lake core is characterized by a floating chronology as the core over-penetrated the sediment-water interface. A Glew core (Glew, 1991) was collected in 2011 to substitute for the missing sediment-water interface. In 2010 a custom designed double-faced freeze corer was deployed in addition to the single faced corer, in order to increase the sediment yield at a given site (Macumber et al., 2012). Freeze cores were sliced at millimeter scale resolution using a custom designed sledge microtome (Macumber et al., 2011). The highest sub-sampling resolution achieved for previous studies had been half-centimeter intervals from Slipper Lake and Lake S41 cores.

3.1.1 Previous work

Eight sites from previous paleolimnological studies located on the Slave Province have been incorporated into the dataset (Table 2.1). The sediment cores from previously published studies were collected using a modified Livingstone corer (Wright et al., 1984), except the Slipper Lake core, which was collected using a modified KB gravity corer and a mini-Glew gravity corer (Glew, 1991; Glew et al., 2001).

3.2 Chronology

Most radiocarbon dates were obtained from bulk sediment samples from material collected along the Tibbitt to Contwyoto Winter Road, as macrofossils are rare in the Subarctic. Samples were analyzed at Queen's University, Belfast (starting with UBA, Table 3.1) and were pretreated with a standard acid wash in to remove non-contemporaneous carbonate material. The analyses were performed using accelerator

mass spectrometer (AMS) dating techniques. Radiocarbon dating of sediments reported in previous work was performed using both AMS and conventional techniques. Radiocarbon ages were calibrated using either Clam (Blaauw, 2010) or Calib software version 6.1.0 (Stuiver and Reimer, 1993); both programs used the IntCal09 calibration curve (Reimer et al., 2009). Radiocarbon ages younger than AD1950 were calibrated in CALIBomb (Reimer et al., 2004) with the NH_zone1.14c dataset (Hua and Barbetti, 2004).

3.3 Classical age-depth modeling with Clam

Smooth spline age-depth models were constructed for sediment cores obtained from the TCWR and previously published studies using the 'classical' age-depth modeling software Clam (Blaauw, 2010) and the IntCal09 calibration curve (Reimer et al., 2009). With the exception of Danny's and Waite lakes, the smoothing parameter was set to 0.3 and the year the core was collected was added as the age of the sediment-water interface. Due to the high density of radiocarbon dates for Danny's and Waite lakes, the smoothing parameter was increased to 0.7 and 0.5, respectively. The core from Lake P39 had only three non-outlying dated horizons so the model was constructed using a linear regression. For Slipper Lake, the three uppermost non-interpolated ^{210}Pb dates were included in the model.

3.4 Outlier analysis

For cores with low dating resolution (typically less than five radiocarbon dates or less than one radiocarbon date per thousand years), suspected outliers were removed on an ad

hoc basis when a radiocarbon date either created a strong age reversal in the model or a strong, anomalous shift in accumulation rate that could not be supported by sedimentological evidence. We also took into account the regional trends to aid with outlier identification. For example, many age-depth models show a pronounced decrease in accumulation rate after about 6000 or 5000 cal yr BP. Only clear outliers were treated and many age-depth models did not have outliers.

The Danny's Lake core has 25 radiocarbon dates over 115 cm of sediment and the age-depth model contains age reversals. A Bayesian outlier analysis was performed using the general outlier model (Bronk Ramsey, 2009a) in OxCal version 4.1 (Bronk Ramsey, 2009b). This model assumes that the outliers are in the time dimension and distributed according to a Student-*t* distribution with 5 degrees of freedom (Christen, 1994; Bronk Ramsey, 2009a). Each radiocarbon date was assigned a 5% probability of being an outlier. The first outlier analysis identified all three dates at the bottom of the core as being outlying so we increased the prior probability of UBA-16439 to 10%, as this date creates the largest age reversal. A subsquent outlier analysis still identified the two bottommost dates as outliers and it was unclear as to which was more likely to be an outlier. We then looked at the age-depth models from other lakes and from previous studies for clues to resolve this problem. As many of the other models support a higher accumulation rate prior to about 6000 cal yr BP we used this information to assign a 10% prior probability to UBA-17932. Further details of the outlier analysis can be found in Appendix B.

The age-depth modeling procedure with the Bayesian statistics software Bacon does not require an outlier analysis as the program models radiocarbon age distributions

using the Student-*t* distribution. This approach produces longer tails than obtained using the Normal model, and the model is robust to the presence of outliers (Blaauw and Christen, 2011).

3.5 Estimation of deposition time

An estimate of average deposition time, in yr/cm (inverse of accumulation rate), is required as *a priori* information to run age-depth models using the Bayesian software Bacon (Blaauw and Christen, 2011). This estimate must be based on prior knowledge, which is obtained from previously built age-depth models from lakes in the region (Goring et al., 2012). Here we use the age-depth models constructed in Clam to calculate the deposition time at 100-year intervals for each model (see Appendix B for detailed instructions). The deposition times between the uppermost non-outlying date and the date used to model the surface age were not included in graphing the deposition times, as there is potential uncertainty with the assumption that the age of the sediment-water interface is the year that the core was collected. This is because the uppermost sediments have much higher water content and therefore can yield anomalously high accumulation rates. Webb and Webb (1988) assumed 50% compaction in sediments below the uppermost 5 to 10 cm of the sediment column based on dry weight/wet weight ratios, yet they found that the accumulation rates were still higher during the historic period. Because dry weight/wet weight data has not been collected for this study, the effect of compaction and dewatering is not taken into account in graphing the deposition times. P39 and Slipper lakes lacked sufficient chronological control and were omitted from the dataset.

3.6 Bayesian age-depth modeling with Bacon

The age modeling procedure for Bacon is similar to that outlined in Blaauw and Christen (2005), but more numerous and shorter sections are used to generate a more flexible chronology (Blaauw and Christen, 2011). Waite, Danny's and Horseshoe lakes all have at least ten non-outlying radiocarbon dates and were deemed suitable for Bayesian modeling with Bacon. Memory or coherence in accumulation rates along the core is a parameter that is defined based on how strongly the accumulation rate at each interval depends on the previous interval. For example, the memory for modeling accumulation in peat sediments should be higher than for lacustrine sediments because accumulation of peat in peat bogs is less dynamic over time than the accumulation of sediments in a lake (Blaauw and Christen, 2011). Here we used the memory properties suggested for lake sediment cores (i.e. a "strength" of 20 and a mean of 0.1). The accumulation rates for Waite, Danny's, and Horseshoe lakes were based on the estimates from chapter 3.5 (20, 70, and 160 yr/cm, respectively) and the accumulation shape for Waite and Horseshoe was set to 2, as suggested by Blaauw and Christen (2011). The accumulation shape controls how much influence the accumulation rate will have on the model. The default value of 2 is fairly low, thus the model has a fair amount of control. For the Danny's lake age model, the accumulation shape was increased to a value of 20 to avoid perturbations in the model caused by known outliers. The step size for Waite Lake was set to 5 cm, which is the default for a lake (Blaauw and Christen, 2011). The Danny's and Horseshoe lakes age-depth models required more flexibility due to the observed sustained (i.e., not due to spurious radiocarbon dates) shifts in accumulation, so step size was lowered to 2 cm.

3.7 Estimate of the Freshwater Reservoir Effect (FRE)

A few of the cores contained macrofossils, but it was not possible to conduct paired dating of bulk sediment with macrofossils or a chronostratigraphic marker such as a tephra or pollen horizon. The presence of a FRE was therefore evaluated by calculating the age of the sediment-water interface through extrapolation of the age-depth model and comparing the modeled age at 0 cm to the year the core was collected. Where differences existed, we assumed an input of old carbon into the system. To model the age at 0 cm, we first removed the data point representing the year the core was collected. We then used a query in Clam (ageofdepth=0) to provide an estimate of the projected age of the sediment-water interface based on the assumption that the accumulation rate at the uppermost dated horizon remained constant. Finally, we added the difference between the year the core was collected and the year 1950 to adjust for the Clam results in BP. Even when a FRE was estimated, we did not apply a correction to our age-depth models. Our focus is to evaluate accumulation patterns across space and time. Application of a FRE correction is not relevant to that objective. A FRE of less than 500 years will not dramatically affect our conclusions; especially since we are sampling accumulation rates at 100-year intervals. Moreover, it is likely that the FRE will change over time (e.g. Barnekow et al., 1998; Geyh et al., 1998; Grimm et al., 2009; Blaauw et al., 2011); it is known that the landscape and vegetation of the study area underwent substantial changes in the time period we are investigating. Without multiple horizons of paired ^{14}C dates and bulk sediments or chronostratigraphic markers of AMS dating on material not likely to be

affected by a FRE (e.g., macrofossils, pollen concentrates) it is not possible to verify a downcore FRE.

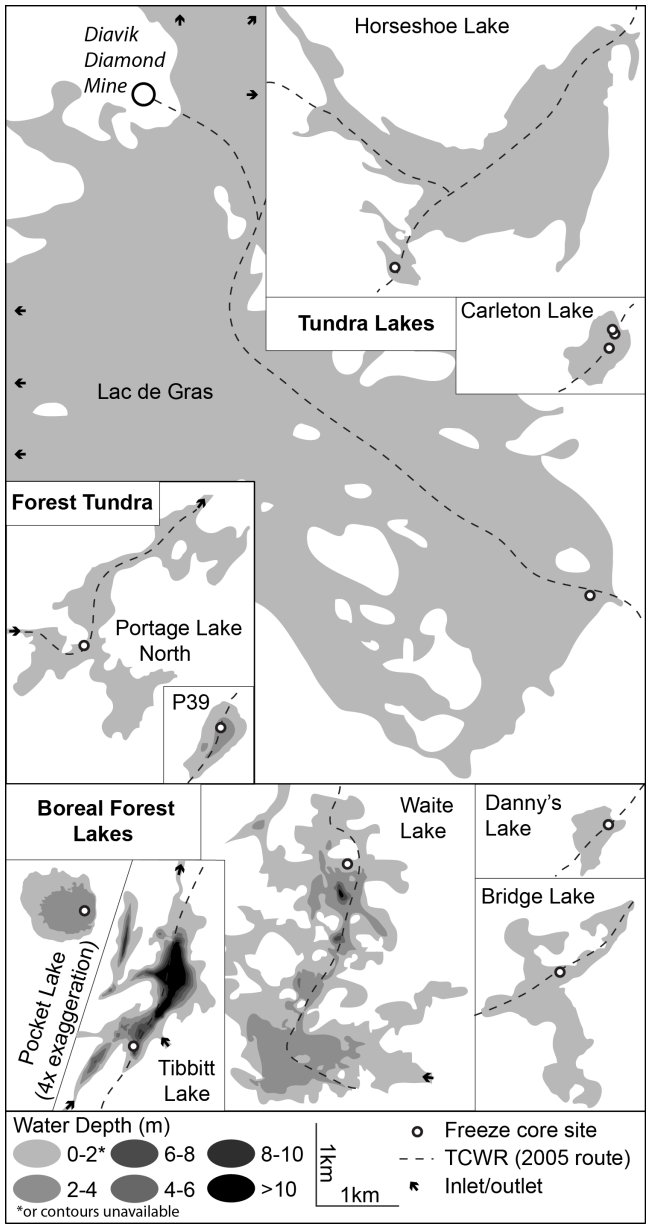

Figure 3.1 Coring sites within the lakes from the TCWR project, with bathymetric contours shown when known. While Lac de Gras is drawn to scale, it is much larger than is shown here as indicated by small arrows. The coring sites of P55_DM1 and P55_DM3 are not shown for this reason.

Table 3.1 Radiocarbon ages from all sites, calibrated with the IntCal09 calibration curve (Reimer et al., 2009) using either Calib software version 6.1.0 (Stuiver and Reimer, 1993) or Clam (Blaauw, 2010). The radiocarbon ages younger than AD1950 (italics) were calibrated in CALIBomb (Reimer et al., 2004) with the NH_zone 1.14c dataset (Hua and Barbetti, 2004). Lakes part of the TCWR project include the portage number along the road (P#) and, for these cores, when the depth is given as a single number the sample has been taken from a mm-thick slice starting at the depth indicated. Outliers are shown in bold. Citations: (1) Moser and MacDonald, 1990; (2) MacDonald et al., 1993; (3) Edwards et al., 1996; (4) Wolfe et al., 1996; (5) Penitz et al., 1999; (6) Huang et al., 2004; (7) Rühland and Smol, 2005; (8) MacDonald et al., 2009; (9) Paul et al., 2010; (10) Galloway et al., 2010; (11) Macumber et al., 2012; (12) Upiter et al., *in press.*

Lab ID	AMS or conv.	Depth range (cm)	^{14}C age (BP) ± 1σ	Material Dated	δ^{13}C ‰ (VDPB)	Cal BP ± 2σ
Pocket Lake *face one of two, collected in 2012 (**new data, will be added to final version)*						
UBA-20676	AMS	10–10.5	362 ± 27	Bulk sed.	-25.1	310–414
UBA-22350	AMS	20–20.5	731 ± 31	Bulk sed.	-27.9	653–727
UBA-20679	AMS	52–52.5	1335 ± 25	Bulk sed.	-27.2	1286–1383
UBA-22351	AMS	57–57.5	1394 ± 30	Bulk sed.	-26.7	1279–1348
UBA-22352	AMS	70–70.5	1725 ± 31	Bulk sed.	-22.4	1556–1708
UBA-20677	AMS	90–90.5	2501 ± 30	Bulk sed.	-19.3	2443–2559
UBA-22353	**AMS**	**110–110.5**	**1516 ± 35**	**Bulk sed.**	**-27.2**	**1333–1518**
UBA-20678	AMS	128.5–129	2966 ± 26	Bulk sed.	-25.6	2916–3016
Pocket Lake *face one of one, collected in 2012*						
UBA-20680	AMS	15.5–16	795 ± 27	Bulk sed.	-26.1	674–760
UBA-22346	AMS	36–36.5	1401 ± 27	Bulk sed.	-27.0	1285–1347
UBA-22347	AMS	63.5–64	2145 ± 31	Bulk sed.	-24.8	2037–2304
UBA-22348	AMS	100–100.5	1715 ± 36	Bulk sed.	-25.2	1543–1706
UBA-22349	AMS	140–140.5	2075 ± 32	Bulk sed.	-24.0	1968–2129
UBA-20681	AMS	179–179.5	3195 ± 26	Bulk sed.	-26.3	3368–3459
Tibbitt Lake (P0)[10,11] *face one of one, collected in 2009*						
UBA-17353	AMS	20–21	67 ± 22	Bulk sed.	-24.3	(-4)–255
UBA-17354	AMS	40–41	1409 ± 20	Bulk sed.	-23.3	1292–1343
UBA-17355	AMS	80–81	2046 ± 26	Bulk sed.	-25.2	1930–2111
Beta-257687	AMS	138–138.5	2390 ± 40	Bulk sed.	-22.6	2338–2696
Waite Lake (P14-2)[11] *Glew core, collected in 2011*						
UBA-18968	*AMS*	*17–17.5*	*1.0562 ± 0.003*	*Bulk sed.*	*-24.4*	*AD1956–1957*
UBA-18969	AMS	27–27.5	309 ± 22	Bulk sed.	-26.6	304–455
UBA-18970	AMS	37–37.5	556 ± 26	Bulk sed.	-21.8	522–637
Waite Lake (P14-2)[10,11] *face one of one, collected in 2009*						
UBA-18474	AMS	0	1084 ± 41	Bulk sed.	-10.3	927–1066
UBA-16433	AMS	16.9	995 ± 24	Bulk sed.	-18.6	800–961
UBA-16434	AMS	29.1	1129 ± 22	Bulk sed.	-18.8	965–1076
UBA-16435	AMS	43.2	1455 ± 23	Bulk sed.	-16.5	1304–1384
UBA-16436	AMS	57.8	1519 ± 22	Bulk sed.	-21.1	1345–1514

Lab ID	AMS or conv.	Depth range (cm)	^{14}C age (BP) ± 1σ	Material Dated	δ^{13}C ‰ (VDPB)	Cal BP ± 2σ
Beta-257686	AMS	66.3	1520 ± 40	Bulk sed.	-18.6	1333–1520
UBA-15638	AMS	109.7	2107 ± 29	Twig	-31.7	1997–2149
Beta-257688	AMS	154	2580 ± 40	Bulk sed.	-18.3	2498–2769
Beta-257689	AMS	185	2920 ± 40	Bulk sed.	-18.0	2955–3210
Beta-257690	AMS	205.1	3460 ± 40	Bulk sed.	-17.2	3633–3838
Bridge Lake (P26-1)[11] *face two of two, collected in 2010*						
UBA-18964	AMS	6.5–7	28 ± 23	Bulk sed.	-30.7	(-4)–244
UBA-22873	AMS	12.5–13	694 ± 26	Bulk sed.	-29.5	565–683
UBA-18965	AMS	18–18.5	1883 ± 23	Bulk sed.	-27.0	1736–1882
UBA-22874	AMS	24.5–25	3782 ± 30	Bulk sed.	-30.2	4082–4246
UBA-22875	AMS	30.5–31	4730 ± 30	Bulk sed.	-29.0	5326–5583
UBA-22876	AMS	34.5–35	5487 ± 31	Bulk sed.	-27.3	6210–6322
UBA-18966	AMS	41.5–42	5816 ± 42	Bulk sed.	-28.9	6501–6727
UBA-22877	AMS	50.5–51	6184 ± 32	Bulk sed.	-25.3	6977–7172
UBA-18967	AMS	59.5–60	6762 ± 32	Bulk sed.	-23.4	7576–7667
UBA-22878	AMS	64–64.5	7025 ± 34	Bulk sed.	-23.8	7788–7941
Danny's Lake (P34)[11] *face two of two, collected in 2010*						
UBA-17359	AMS	5.7	693 ± 21	Bulk sed.	-27.5	567–679
UBA-17360	AMS	10.2	855 ± 23	Bulk sed.	-30.1	695–795
UBA-16543	AMS	15–15.5	1329 ± 23	Bulk sed.	-26.3	1184–1299
UBA-17361	AMS	21.9	1617 ± 25	Bulk sed.	-29.2	1416–1556
UBA-17431	AMS	27.8	1659 ± 21	Bulk sed.	-27.8	1521–1615
UBA-16544	AMS	32.6	1916 ± 25	Bulk sed.	-27.5	1818–1904
UBA-20377	AMS	33.5	2071 ± 24	Bulk sed.	-24.7	1987–2120
UBA-20378	AMS	34.2	2159 ± 24	Bulk sed.	-27.8	2061–2305
UBA-17929	AMS	34.5	2257 ± 26	Bulk sed.	-30.2	2158–2343
UBA-20376	**AMS**	**35.3**	**2073 ± 28**	**Bulk sed.**	**-29.5**	**1986–2124**
UBA-20375	AMS	36.8	2248 ± 25	Bulk sed.	-29.5	2158–2339
UBA-17432	**AMS**	**37.6**	**2659 ± 32**	**Bulk sed.**	**-29.0**	**2742–2884**
UBA-20374	AMS	38.4	2392 ± 25	Bulk sed.	-27.6	2345–2488
UBA-20373	AMS	39.3	2448 ± 33	Bulk sed.	-29.1	2358–2702
UBA-17930	AMS	40.4	2549 ± 26	Bulk sed.	-28.6	2503–2748
UBA-20371	AMS	41.4	2554 ± 28	Bulk sed.	-28.7	2503–2750
UBA-20372	**AMS**	**43.3**	**4863 ± 29**	**Bulk sed.**	**-24.7**	**5583–5652**
UBA-16545	AMS	45–45.5	2912 ± 24	Bulk sed.	-29.1	2964–3157
UBA-16546	AMS	56.9	3604 ± 25	Bulk sed.	-26.2	3845–3975
UBA-16547	AMS	70.1	5039 ± 51	Bulk sed.	-29.6	5661–5903
UBA-16548	AMS	85–85.5	5834 ± 29	Bulk sed.	-31.3	6560–6733
UBA-17931	AMS	89.5	6231 ± 34	Bulk sed.	-29.6	7016–7253
UBA-16439	**AMS**	**95.5**	**8112 ± 32**	**Bulk sed.**	**-27.3**	**8997–9125**
UBA-17932	**AMS**	**99.1**	**7623 ± 38**	**Bulk sed.**	**-28.9**	**8370–8518**
UBA-16440	AMS	113.6	7450 ± 30	Bulk sed.	-24.9	8191–8346

Lab ID	AMS or conv.	Depth range (cm)	^{14}C age (BP) ± 1σ	Material Dated	δ^{13}C ‰ (VDPB)	Cal BP ± 2σ
Lake P39[11] *face one of two, collected in 2010*						
UBA-17344	**AMS**	**10–10.5**	**3597 ± 26**	**Bulk sed.**	**-29.1**	**3840–3973**
UBA-17345	AMS	19–19.5	3701 ± 24	Bulk sed.	-28.4	3974–4144
UBA-17346	AMS	29–29.5	5385 ± 35	Bulk sed.	-24.8	6018–6284
Toronto Lake[2,4,5] *Livingstone core, collected in 1987*						
Beta-49705	conv.	35–50	1760 ± 90	Bulk sed.		1421–1887
Beta-53129	conv.	80–85	4200 ± 80	Bulk sed./moss		4450–4956
Beta-53130	conv.	125–130	5460 ± 90	Bulk sed./moss		6001–6408
Beta-49708	conv.	155–160	7040 ± 120	Bulk sed.		7657–8155
Portage Lake North (P47)[11] *face two of two, collected in 2010*						
UBA-17933	AMS	6.5–7	772 ± 24	Bulk sed.	-22.7	673–729
UBA-17159	AMS	13.5–14	4218 ± 38	Bulk sed.	-21.5	4626–4854
UBA-17160	**AMS**	**41–41.5**	**4885 ± 37**	**Bulk sed.**	**-22.2**	**5584–5710**
UBA-17161	AMS	63–63.5	5333 ± 35	Bulk sed.	-25.8	5997–6264
UBA-17162	AMS	86.5–87	5878 ± 34	Bulk sed.	-23.5	6637–6783
Waterloo Lake[2] *Livingstone core, collected in 1987?*						
TO-3312	**AMS**	**28–31**	**4030 ± 50**	**Bulk sed.**		**4413–4801**
TO-3311	AMS	54–56	4640 ± 50	Bulk sed.		5090–5577
TO-3310	AMS	61–63.5	5300 ± 50	Bulk sed.		5939–6257
TO-3313	AMS	75–77	7640 ± 100	Moss		8206–8627
Lake S41[8] *Livingstone core, collected in 2005*						
UCI-25833	AMS	7–7.5	375 ± 15	Bulk sed.		331–499
UCI-25841	AMS	13.4–14	1045 ± 20	Bulk sed.		926–1042
UCI-25836	AMS	23–23.5	1985 ± 15	Bulk sed.		1892–1987
UCI-25835	AMS	32.5–33	2765 ± 20	Bulk sed.		2789–2924
Queen's Lake[1-5] *Livingstone core, collected in 1987?*						
WAT-1770	conv.	15–20	3820 ± 60	Bulk sed.		4010–4414
WAT-1771	conv.	45–50	5600 ± 60	Bulk sed.		6291–6493
WAT-1772	conv.	60–65	6150 ± 60	Bulk sed.		6888–7241
WAT-1773	conv.	100–105	7150 ± 70	Bulk sed.		7842–8159
TO-827	AMS	105	7470 ± 80	Twig		8060–8417
McMaster Lake[1,2] *Livingstone core, collected in 1987?*						
TO-766	**AMS**	**10–12**	**3690 ± 50**	**Bulk sed.**		**3888–4212**
TO-158	AMS	20–22	3680 ± 60	Bulk sed.		3849–4220
TO-767	AMS	30–32	5120 ± 60	Bulk sed.		5730–5990
TO-156	AMS	40–42	5360 ± 60	Bulk sed.		5998–6279
TO-154	AMS	60–62	6180 ± 60	Bulk sed.		6943–7248
UCLA Lake[6] *Livingstone core, collected in ?*						
TO-8840	AMS	20–21	2370 ± 50	Bulk sed.		2319–2698
TO-8842	AMS	35–35.5	4130 ± 50	Bulk sed.		4527–4824
TO-8844	AMS	45–45.5	5680 ± 70	Bulk sed.		6317–6635
TO-8845	AMS	50–50.5	6280 ± 70	Bulk sed.		7002–7413
TO-8846	AMS	55.5–56	7040 ± 70	Bulk sed.		7707–7978

Lab ID	AMS or conv.	Depth range (cm)	^{14}C age (BP) ± 1σ	Material Dated	δ^{13}C ‰ (VDPB)	Cal BP ± 2σ
TO-8847	AMS	64.5–65	7680 ± 70	Bulk sed.		8382–8590
TO-8848	AMS	69.5–70	7960 ± 80	Bulk sed.		8605–9006
Carleton Lake (P49-1A)[11] *face two of two, collected in 2010*						
UBA-19464	**AMS**	**9.5–10**	**2794 ± 34**	**Bulk sed.**	**-25.5**	**2791–2970**
UBA-20002	**AMS**	**15–15.5**	**2778 ± 26**	**Bulk sed.**	**-26.4**	**2793–2950**
UBA-20003	AMS	25–25.5	2716 ± 33	Bulk sed.	-30.1	2757–2868
UBA-19465	AMS	32.5–33	3124 ± 41	Bulk sed.	-27.7	3254–3443
UBA-19466	AMS	40.5–41	3616 ± 37	Bulk sed.	-19.7	3835–4075
UBA-19467	AMS	66.5–67	4927 ± 38	Bulk sed.	-22.8	5594–5728
Carleton Lake (P49-1B)[11,12] *face one of one, collected in 2012*						
UBA-18472	*AMS*	*0–0.5*	*1.0264 ± 0.0035*	*Bulk sed.*	*-27.0*	*AD1955-1957*
UBA-17934	AMS	10–10.5	1046 ± 24	Bulk sed.	-28.0	925–983
UBA-17347	AMS	19.5–20	1925 ± 25	Bulk sed.	-28.7	1822–1926
UBA-17935	AMS	40–40.5	2762 ± 35	Bulk sed.	-28.1	2780–2946
UBA-17348	AMS	64.5–65	3675 ± 24	Bulk sed.	-24.4	3926–4087
UBA-17936	AMS	80–80.5	4635 ± 32	Bulk sed.	-25.7	5304–5465
UBA-17349	AMS	100–100.5	5663 ± 26	Bulk sed.	-24.0	6399–6497
Carleton Lake (P49) *face two of two, collected in 2012*						
UBA-20612	AMS	10.0	702 ± 39	Bulk sed.	-31.7	560–699
UBA-20613	AMS	36.2	1337 ± 31	Bulk sed.	-27.4	1181–1305
UBA-20614	AMS	55.3	1302 ± 46	Bulk sed.	-34.4	1132–1304
UBA-20615	AMS	81.5	2132 ± 31	Bulk sed.	-20.2	2002–2299
UBA-20616	AMS	117.8	2944 ± 32	Bulk sed.	-21.2	2989–3216
Horseshoe Lake (P52-1)[11] *face two of two, collected in 2010*						
UBA-17350	AMS	9–9.5	178 ± 25	Bulk sed.	-29.1	(-2)–291
UBA-17163	AMS	18–18.5	1148 ± 42	Bulk sed.	-28.0	967–1172
UBA-17351	AMS	28–28.5	2763 ± 22	Bulk sed.	-22.5	2785–2924
UBA-17352	AMS	38–38.5	3343 ± 23	Bulk sed.	-25.7	3481–3639
UBA-19973	AMS	43.2	3776 ± 36	Bulk sed.	-28.8	3992–4281
UBA-17938	AMS	46–46.5	4885 ± 27	Bulk sed.	-27.6	5589–5653
UBA-17165	AMS	55–55.5	5916 ± 58	Bulk sed.	-23.6	6628–6897
UBA-17937	AMS	68–68.5	6723 ± 29	Bulk sed.	-27.1	7516–7656
UBA-17166	AMS	80–80.5	7488 ± 40	Bulk sed.	-25.5	8199–8383
UBA-17167	AMS	106–106.5	8011 ± 43	Bulk sed.	-22.8	8718–9014
Lac de Gras (P55)[11] *face two of two, collected in 2010*						
UBA-17939	AMS	12–12.5	1123 ± 23	Bulk sed.	-29.2	965–1067
UBA-17356	**AMS**	**19–19.5**	**3299 ± 38**	**Bulk sed.**	**-26.9**	**3447–3631**
UBA-17357	AMS	32–32.5	1607 ± 29	Bulk sed.	-21.5	1412–1551
UBA-17358	AMS	46–46.5	2144 ± 35	Bulk sed.	-25.2	2003–2305
Lac de Gras (P55_DM1) *collected in 2012*						
D-AMS 001550	AMS	10–11	784 ± 23	Bulk sed.	-27.1	677–732
D-AMS 001551	AMS	20–21	1797 ± 23	Bulk sed.	-26.9	1629–1817
D-AMS 001552	AMS	30–31	2636 ± 25	Bulk sed.	-27.0	2738–2781
D-AMS 001553	AMS	40–41	3590 ± 27	Bulk sed.	-26.8	3836–3972

Lab ID	AMS or conv.	Depth range (cm)	^{14}C age (BP) ± 1σ	Material Dated	δ^{13}C ‰ (VDPB)	Cal BP ± 2σ
Lac de Gras (P55_DM3) *collected in 2012*						
D-AMS 001554	AMS	10–11	1719 ± 23	Bulk sed.	-26.1	1561–1696
D-AMS 001555	AMS	20–21	3459 ± 26	Bulk sed.	-26.0	3642–3828
D-AMS 001556	AMS	30–31	5509 ± 28	Bulk sed.	-25.9	6223–6396
D-AMS 001557	AMS	40–41	7827 ± 31	Bulk sed.	-24.3	8543–8696
Slipper Lake[7] *KB gravity and mini-Glew, collected in 1997*						
^{210}PB Age	n/a	0	n/a	Bulk sed.	n/a	(-49)–(-45)
^{210}PB Age	n/a	2	n/a	Bulk sed.	n/a	6–20
^{210}PB Age	n/a	3	n/a	Bulk sed.	n/a	34–94
TO-9671	AMS	21.5–22.5	3270 ± 80	Bulk sed.		3359–3688
TO-9672	AMS	43.5–44.5	4760 ± 70	Bulk sed.		5321–5603
Lake TK-2[9] *Livingstone core, collected in 1996*						
Beta-167871	AMS	32–34	2480 ± 40	Bulk sed.		2365–2718
Beta-167872	AMS	60–62	3870 ± 40	Bulk sed.		4157–4416
Beta-167873	AMS	96–98	5670 ± 40	Bulk sed.		6322–6558
TO-7871	AMS	132	7370 ± 80	Twigs		8020–8349
TO-7870	AMS	137	7190 ± 80	Twigs		7860–8178
TO-7869	AMS	142	7740 ± 90	Twigs		8375–8772
TO-7868	AMS	174	7780 ± 70	Twigs		8412–8761

4. Results

The radiocarbon results from all sites included in this study, along with the results from the outlier analysis are summarized in Table 3.1. We use the term 'site' instead of 'lake' because multiple cores were obtained from some lakes. The year the core was collected is included in Table 3.1 because it was used to model the age of the sediment-water interface in the Clam age-depth models. The age-depth models derived using Clam (Fig. 4.1) were ordered from the southern-most lake in the top left to the northern-most lake in the bottom right. The inclusion of previous results is intended to improve perspective on regional trends and is in no way intended to replace published models. The results of sampling accumulation rates at 100-year intervals from the Clam age-depth models are shown in Figure 4.2.

4.1 Sites with rapid accumulation rates (<40 yr/cm)

Rapid sediment accumulation rates are described as less than 40 yr/cm. Sediment cores modeling to be in this category are Pocket, Tibbitt, Waite, Carleton-2012, and Lac de Gras. Due to rapid accumulation, these 1 to 2 m core records only extend back to ~ 3500 cal yr BP at most. The cores in this category yield internally consistent age-depth models with the exception of one radiocarbon date that is a clear outlier in the Lac de Gras core (Fig. 4.1).

The lakes in this category have deposition times between 10 and 40 yr/cm (= ~ 25 yr/cm) based on 107 radiocarbon measurements that followed a normal distribution (Fig. 4.2a). The accumulation pattern for Tibbitt Lake is different from the others as it increases steadily from 5 yr/cm at 2500 cal yr BP to 50 yr/cm at the top, but the very

rapid deposition near the bottom overlaps a plateau in the IntCal09 calibration curve known as the Hallstatt Plateau (ca 2700-2300 BP; Blockley et al., 2007). Plateaus in the calibration curve cause radiocarbon dates to calibrate to the same age, even though the uncalibrated ages are hundreds of years different. Waite Lake core has the steadiest accumulation pattern with a deposition time of 20 yr/cm at the bottom (~3500 cal yr BP) rising gradually to about 10 yr/cm at the top. The accumulation rate of both Lac de Gras core and Carleton-2012 increases sharply around 1500 cal yr BP and then decreases around 1300 cal yr BP, creating a "dip" in the accumulation rate (Fig. 4.2b). This pattern is also observed in the Danny's Lake age-depth model.

There were cores from sites in both Carleton Lake and Lac de Gras that display intra-lake variation in sedimentary style. At Carleton Lake, one core is characterized by a high sedimentation rate, while the other two are characterized by a moderate accumulation rate. At Lac de Gras, all three collected cores were characterized by different accumulation rates: slow, medium and fast. This variability is to be expected from very large lakes with multiple depocentres such as Lac de Gras. However, the presence of different sedimentation rates in the very small Carleton Lake (30 ha) indicates how variable sedimentation rates can be, even within one basin (e.g. Schiefer, 2006).

4.2 Sites with moderate accumulation rates (40 – 110 yr/cm)

The sites in this category are Danny's, Toronto, S41, Carleton-1A, Carleton-1B, P55_DM1, and TK-2. Three of the cores in the moderate accumulation rate category are characterized by a sedimentary record that extends just beyond 8000 cal yr BP. The other

four cores in this category have records that extend back between 4000 and 6000 years (Fig. 4.1).

The outlier analysis performed in OxCal identified five outliers in the Danny's Lake core, which were omitted from the smooth spline age-depth model constructed with Clam. Four of the five outliers were older than the model and the fifth was only slightly younger. For Carleton-1A, the upper three radiocarbon dates, at 9.5, 15 and 25 cm, all overlapped within the age range of 2900 to 2700 cal yr BP. For this reason the uppermost two dates were omitted from the age-depth model constructed in Clam. The overlap may have been an artifact of calibration from the Hallstatt Plateau (Blockley et al., 2007), or may have been the result of sediment mixing. According to the linear-derived accumulation rate of 68 years/cm suggested by the oldest four dates, the date at the very top of the core (9.5 cm) should be younger than 2000 cal BP, which is well outside the range of the plateau. The core from Lake TK-2 has an age reversal within the bottommost four dates. Because these dates were obtained from twigs, the reversal is likely due to older organic material being washed into the basin (e.g., delayed deposition). Clam was able to accept the reversal as the date was within error of the others.

The lakes in this category accumulated at rates between 40 and 110 yr/cm (= ~ 70 yr/cm) (Fig. 4.2). The histogram has a bimodal distribution with a primary mode at ~60 yr/cm and a secondary mode at ~100 yr/cm. Most of the lakes in this category were characterized by fluctuations in accumulation rate. Danny's Lake, which had the highest dating resolution of all the cores, was characterized by a deposition rate of 45 yr/cm shortly before 8000 cal yr BP, which incrementally decreased to a rate of 110 yr/cm by 5000 cal yr BP. This transition corresponds to a shift in sedimentation from minerogenic-

rich at the base of the core to organic-rich sediment above. After 5000 cal yr BP the accumulation rate increased again to a deposition rate of 40 yr/cm by 1500 cal yr BP, followed by a slowing to 80 yr/cm by 700 cal yr BP. Carleton-1B also has a highly variable sedimentation rate that mimics the patterns at Danny's Lake, except during the last 2000 years. The accumulation rate fluctuated from 55 yr/cm at 6500 cal yr BP, to ~80 yr/cm by 5000 cal yr BP, to just above 40 yr/cm at 3000 cal yr BP, then increased again to around 90 yr/cm at the top of the core.

Lake TK-2 was characterized by a similar sedimentation pattern to Danny's and Carleton lakes between 8500 and 6000 cal yr BP (e.g. an initial rapid deposition rate less than 30 yr/cm, which is somewhat of an artifact of the age reversal discussed above), slowing to a deposition rate of ~60 yr/cm by 6000 cal yr BP. By 3000 cal yr BP, the deposition rate stabilized at ~ 70 yr/cm.

Toronto Lake does not follow trends similar to the other cores in this category as the accumulation is fairly consistent, starting at 47 yr/cm around 8000 cal yr BP, increasing to ~40 yr/cm by 6000 cal yr BP, then slowing to ~60 yr/cm between 3000 and 2000 cal yr BP. The remaining lakes in this category, S41, Carleton-1A, and P55_DM1 are all characterized by fairly short sedimentary records (<3000 years), and thus cannot be compared to the long-term patterns of the other lakes.

4.3 Sites with slow accumulation rates (100 – 250 yr/cm)

The sites in the slow accumulation category are Bridge, Waterloo, UCLA, Horseshoe, and P55_DM3. All five sites in this category extend back to 8000 cal yr BP or beyond.

The models are internally consistent, with only one outlier from the Waterloo Lake age-depth model, which is older than the model (Fig. 4.1).

Accumulation rates range between 100 and 250 yr/cm (Fig. 4.2). The histogram is multi-modal, reflecting high variability within this category. The main observed pattern occurs during about 8000 to 5000 cal BP, whereby Bridge, UCLA, and Horseshoe lakes are all characterized by a reduction in accumulation rates. This rate change was linked to changes in sediment source, which changed from minerogenic-rich at the based of the core to organic-rich above. For Bridge Lake, the deposition time increases steadily from ~50 yr/cm at 7600 cal yr BP to 200 yr/cm at 4000 cal yr BP. The sedimentation rate change is linked to a distinct color change at ~4200 cal yr BP, where the light brown sediments characterizing the basal portion of the core, abruptly transition to a dark, organic-rich unit at the top. The depositional rate is constant at ~200 yr/cm until 2500 cal yr BP and steadily decreases to 160 yr/cm by 100 cal yr BP. For UCLA Lake, the deposition rate increased from 65 yr/cm at 8700 cal yr BP to 180 yr/cm by 6000 cal yr BP, followed by a steady decrease in depositional rate to 140 yr/cm by 2500 cal yr BP. P55_DM3 has the slowest accumulation rate of all lakes examined; it yields a deposition rate of greater than 200 yr/cm at 8000 cal yr BP, increasing to 250 yr/cm, at 5000 cal yr BP, and then declining toward the top, where it stabilizes at 180 yr/cm by 1500 cal yr BP.

The accumulation rate profile for Horseshoe Lake displayed the highest variability of any studied profile. Modeled deposition rates are low (~20 yr/cm) between 8700 – 7500 cal yr BP and then increased to 225 yr/cm by 5000 cal yr BP. The transition around 7500 cal yr BP is associated with a shift from minerogenic-rich sediment at the core bottom to organic-rich sediment above. Above ~7500 cal yr BP, the deposition rate

again gradually decreases to 100 yr/cm by 3000 cal yr BP, then increases to 150 yr/cm by 2000 cal yr BP and finally decreases again to 60 yr/cm at the core top.

4.4 Sites with poor chronological constraint

Some sites did not easily fit into the other three categories, either due to lack of dating resolution (P39 and Slipper) or because the accumulation profile is characterized by a dramatic shift in accumulation rate (Portage North, Queens, and McMaster; Fig. 4.2). P39, Portage North, and McMaster lakes all had one outlier – identified on an ad hoc basis – that fell between 4000 and 5000 cal yr BP (Fig. 4.1). For P39, the uppermost radiocarbon date we determined to be an outlier. Because the core was collected in only 110 cm water depth, the top of the core was most likely disturbed due to the yearly winter freezing of ice to the sediment-water interface. No further research was undertaken on this core and accumulation rates were not estimated. As Slipper Lake lacked sufficient chronological control (based on two radiocarbon dates and a ^{210}Pb profile), it was also omitted from calculations of accumulation rate. Portage Lake North, Queens Lake and McMaster Lake had accumulation patterns that appeared sensitive to Hypsithermal warming between 8000 and 5000 cal yr BP (Fig. 4.2). Portage Lake North had a deposition time of 20 yr/cm at 6600 cal yr BP, which steadily slowed to 110 yr/cm by 5000 cal yr BP. Queen's Lake had a deposition time of 25 yr/cm at 8000 cal yr BP, which steadily slowed to 132 yr/cm by 4500 cal yr BP. Similarly, McMaster had a DT of 34 yr/cm at 7000 cal yr BP, which slowed to 170 yr/cm by 4200 cal yr BP.

4.5 Bayesian age-depth modeling

Figure 4.3 shows age-depth models derived from Bacon software using Bayesian statistics for each lake along with three plots per model that describe: (1) the stability of the model (log objective vs. iteration); (2) the prior (green line) and posterior (grey filled) accumulation rate (middle), and; (3) the prior and posterior memory properties (bottom). Each Bayesian model was compared to the model constructed using Clam (thin, black line in Fig. 4.3).

The Bayesian model from Waite Lake was very stable most likely because it covered a shorter time period and there were not as many shifts in accumulation. Danny's Lake also yielded a very stable model, keeping in mind that the weight on accumulation rate was set very high. Both Waite and Danny's lakes models showed high agreement with the models constructed in Clam. The model for Horseshoe Lake showed the highest degree of instability, which can be seen in the fluctuations in the iteration plot as well as the age-depth model, where above 80 cm the model "runs away". We reduced the strength of the accumulation rate prior to a value of 1 and reduced the memory mean to a value of 15 to moderate this effect, but the model still has a high degree of instability. The Bayesian model for Horseshoe Lake deviates from the Clam model by up to hundreds of years, especially where the Bayesian model has been more flexible around a shift in accumulation. One of the more dramatic offsets was through the interval between ~ 4000 and 6000 cal yr BP. The Clam model was smooth through this period, whereas the Bayesian model suggested there might have been a hiatus in sediment deposition.

All three models were characterized by posterior distributions of accumulation rate that match the prior. This outcome is to be expected because the strength of the prior was set low. Danny's and Horseshoe lakes also had a good agreement with prior and

posterior memory properties. However, at Waite Lake the model employed more memory than was suggested by the prior information.

4.6 Freshwater Reservoir Effect (FRE)

For the few cores where macrofossils were available, the macrofossil dates agree well with ^{14}C ages on bulk sediments. The Waite Lake core over-penetrated the sediment-water interface, so a Glew core was extracted to capture the uppermost sediments of this lake. A ^{14}C date at 17 cm from the Glew core yielded a modern age of AD1956, which would confirm the absence of a FRE for Waite Lake at the top of the core. Further down the core, a twig date at 110 cm (UBA-15638) aligns with the model constructed otherwise on bulk dates, thus confirming the absence of a FRE in this section of the core. For the Queen's Lake core, a horizon with paired macrofossil and bulk sediment dating is located below the shift in sedimentation from minerogenic-rich at the bottom to organic-rich sediments at the top. Although the paired dating suggests no FRE, this result cannot support the absence of a FRE in the overlying organic-rich sediments. The bottommost four dates in the TK-2 core are from twigs. Unfortunately there are no bulk dates in this part of the core so it is not possible to assess the presence or absence of a FRE, and similar to the situation in the Queens Lake core, the twig dates lie below a change in sedimentation from organic-poor sediment at the bottom to organic-rich sediment above. Interestingly, while macrofossils are very uncommon, two of the cores have them in sediment horizons characterized by low organic content. This suggests that either the macrofossils were more abundant at that time or the preservation potential was higher in the minerogenic-rich sediment than in the organic-rich sediment.

Using the extrapolation method in Clam, the FRE estimate for Queen's Lake does not add up because the assumption of a linear accumulation rate at the top is not supported by the other dates, which follow a non-linear curve in this section. When the year the core was collected is removed, the model changes substantially. Under this scenario the projected age of the sediment-water interface is 3000 years, which we do not believe to be a FRE based on paired dating.

The FRE estimate for Danny's Lake is modeled to be 430 years. We know that the top is present because the sediment-water interface was captured and, although the ^{210}Pb results did not reach background (unpublished data), the values did indicate that the sediments at the surface are modern. For the Lac de Gras (P55) core, the modeled age of the sediment-water interface is ~600 cal yr BP. Although this date is suggestive of a FRE, it is more likely due to mixing at the top of the core, indicated by mm- to cm-scale rip-up clasts of semi-consolidated sediment floating in a red sediment-water mix.

The Pocket Lake core has a distinct off-white wisp of minerogenic-rich sediment at 55 cm, which has been identified by microprobe analysis as tephra shards (unpublished). The age-depth model places this horizon at ~1390 cal yr BP and it is believed to be the White River Ash (c.f. Robinson, 2001; Lerbekmo, 2008; Pyne-O'Donnell et al., 2012), which has an age of 1147 cal BP (Clague et al., 1995). However, the age presented by Clague et al. (1995) should be updated based on the IntCal09 calibration curve. In future work, we will pursue using this horizon as a chronostratigraphic marker as well as using it as a method for assessing the freshwater reservoir effect.

Figure 4.1 (page 42) Age-depth models constructed using a smooth spline regression in Clam for all 22 sites, listed from south (top left) to north (bottom right). Radiocarbon dates, calibrated with IntCal09 (Reimer et al., 2009), are shown in blue, the year the core was collected representing the age of the sediment-water interface is shown in green, outliers are red, and the 95% confidence interval is grey. The scale for Waite Lake is to be used as a relative measure only as the freeze corer over-penetrated. The sediment-water interface for P39 is shown for illustrative purposes only and we have little confidence in this data point or age-depth model.

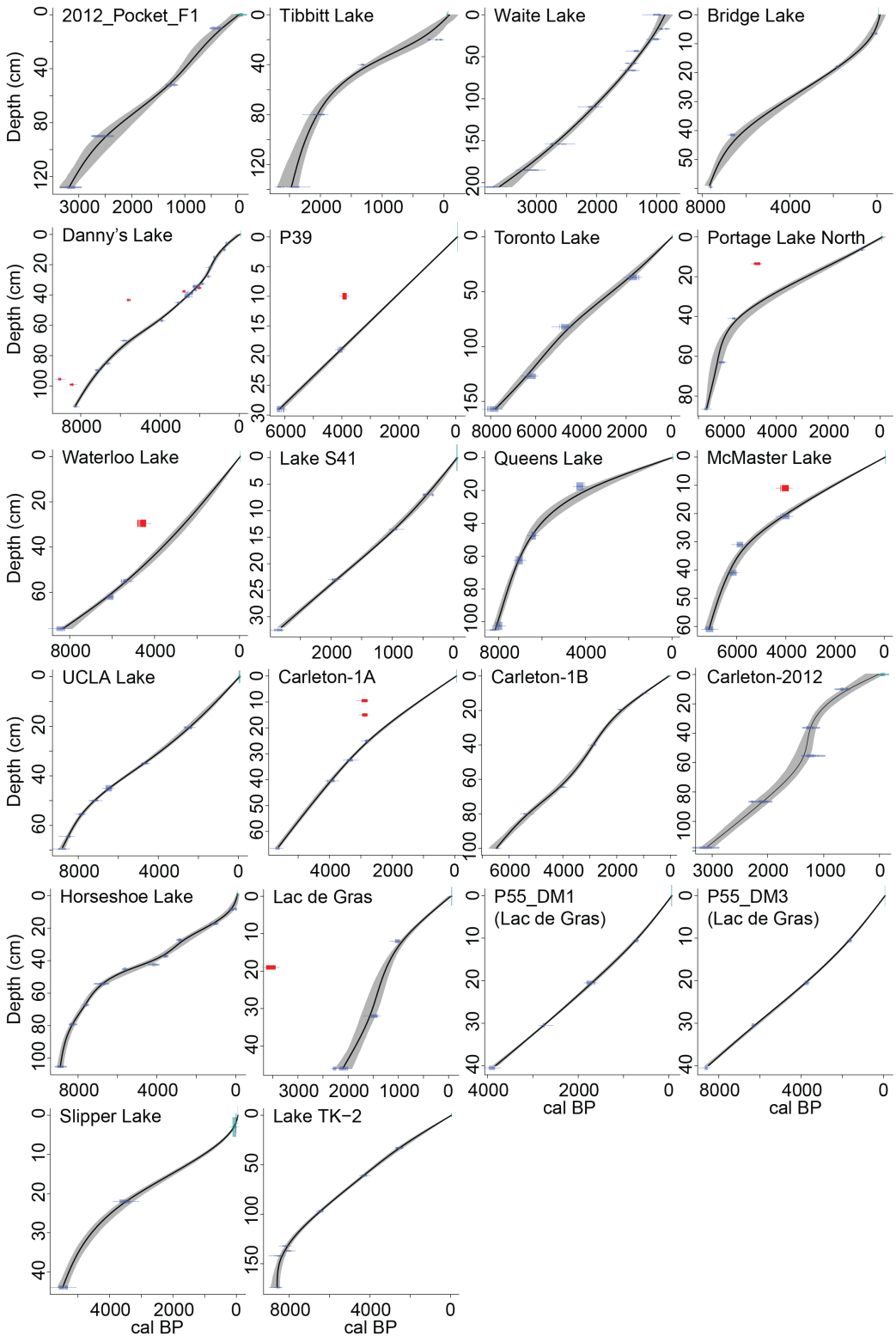
2012_Pocket_F1
Tibbitt Lake
Waite Lake
Bridge Lake
Danny's Lake
P39
Toronto Lake
Portage Lake North
Waterloo Lake
Lake S41
Queens Lake
McMaster Lake
UCLA Lake
Carleton-1A
Carleton-1B
Carleton-2012
Horseshoe Lake
Lac de Gras
P55_DM1 (Lac de Gras)
P55_DM3 (Lac de Gras)
Slipper Lake
Lake TK−2
Depth (cm)
cal BP

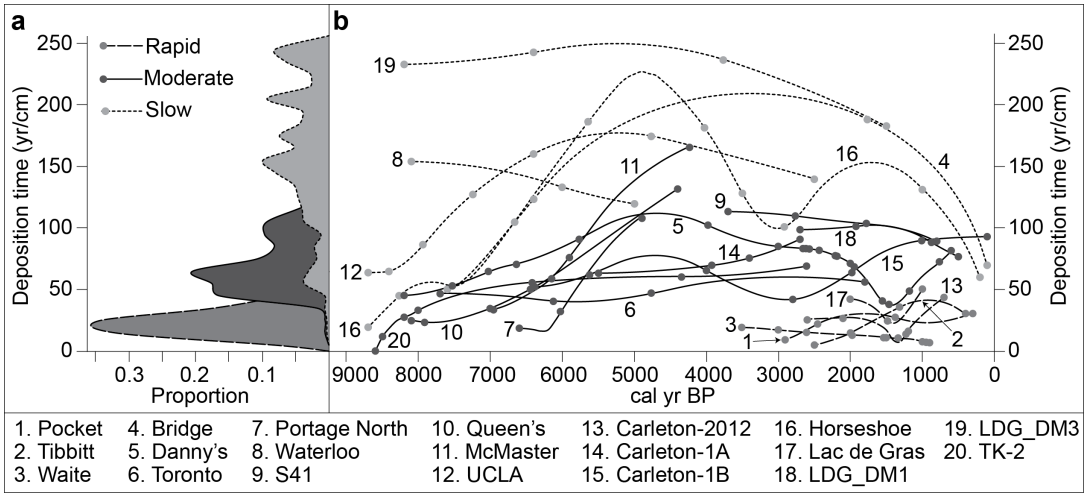

Figure 4.2 (a) Histogram of accumulation rates from rapid, moderate, and slowly accumulating lake site categories, sampled at 100-year intervals from the age-depth models constructed in clam. (b) Accumulation rate profiles for each site showing fluctuations over time and the variability between lake sites.

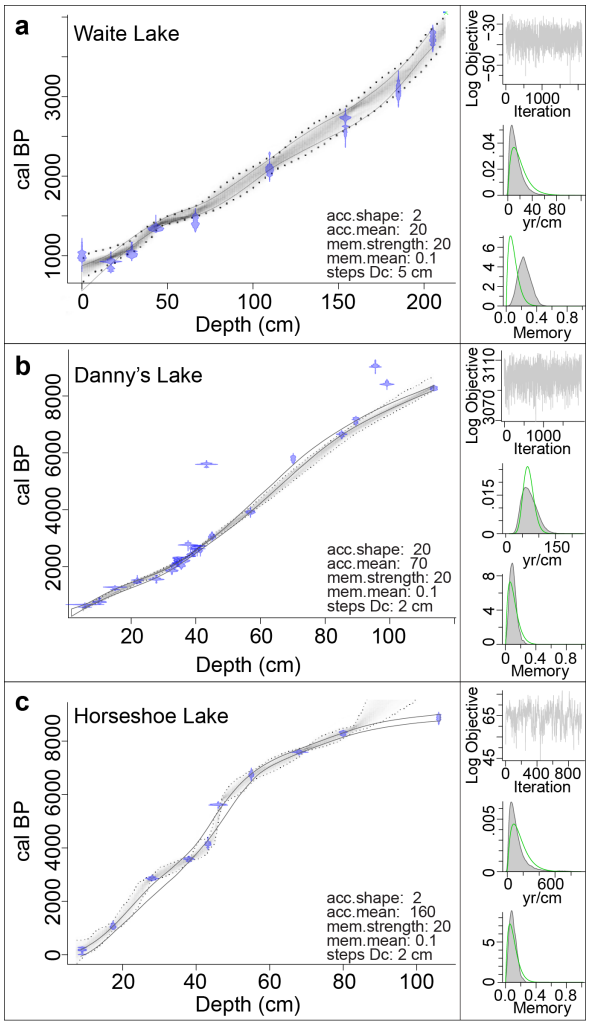

Figure 4.3 Bayesian age-depth models constructed with the age-depth modeling software Bacon. (a) Waite Lake, (b) Danny's Lake, and (c) Horseshoe Lake. Blue shapes are radiocarbon dates and the grayscale on the model represents the likelihood, where the darker the grey, the more likely the model is of running through that section. The outer, dotted black line is the 95% confidence interval. Thin, black, solid lines on the model are the 95% confidence interval from the Clam model. On the right hand side of each model are three plots: (top) stability of the model; (middle) prior (green) and posterior (grey, filled) distributions of accumulation mean; and (bottom) prior and posterior distributions of memory properties.

5. Discussion

5.1 Spatial variability in accumulation rates

The three southernmost boreal forest lakes (Pocket, Tibbitt, and Waite) are substantially further south of the treeline and closer to Great Slave Lake than the other two lakes in the boreal forest zone (Bridge and Danny's; Fig. 2.1). As would be expected, Pocket, Tibbitt and Waite Lake are three of the five lakes with the highest accumulation rates, suggesting that the accumulation rate can be related to in-lake productivity and in-wash of organic detritus.

Bridge and Danny's lakes are also located south of the modern-day treeline, but both sites accumulate at slower rates than the three lakes discussed above. The last 3000 years of accumulation at Danny's lake mirrors the pattern of rapidly accumulating sites, but is slower by about 10-20 yr/cm. This suggests that Danny's lake responds similarly to the southernmost lakes, but may either be slightly less productive due to colder temperatures at a location closer to the polar front, or judging by the bathymetry (Fig. 5.1), the coring site itself may receive less sediment than the main basin in the lake. The latter is likely, as was shown in a study of a B.C. lake by Schiefer (2006), that sedimentation rates can change dramatically across a single basin. The accumulation rate at Bridge Lake is extremely slow and again we look at the bathymetry for an explanation (Fig. 5.1). The coring location for Bridge Lake is nestled into a steep slope, proximal to a deeper sub-basin with a much thicker sediment package so most likely sediment is bypassing the coring location. Based on the second reflector within this package (Fig.

5.1) that we interpret as sediments of glacial origin based on recovery of a centimeter thick band of inorganic grey-white clay in the freeze core, sediments in the basin are at least 2 m thicker than at the coring site due to sediment focusing.

As stated above, three of five rapidly accumulating lakes were located in the boreal forest zone while the other two are found in the tundra. These other two sites are Carleton-2012 and Lac de Gras. Examination of the bathymetry profiles reveals certain basin features that could explain the rapid accumulation rates (Fig. 5.1). Carleton Lake has a shallow shelf over 500 m long that has a maximum depth of two meters, a slope covering less than 100 m, and a main basin that is about 500 m long at a depth of about 4 m. The Carleton-2012 freeze core was collected from a site closer to the slope and shelf than the Carleton-1A and Carleton-1B freeze cores. The shelf, which sits at two meters water depth, may be susceptible to re-suspension of fine detritus due to surface waves touching bottom generated during windy or stormy conditions. The re-suspended sediments would be transported down into the basin, with the majority being deposited closer to the slope terminus. The Lac de Gras coring site is along a drop-off and the landscape has higher relief than the majority of the sites in this study so, in this case, the high accumulation rate can be related to topographic relief. Figure 5.2 is a summer photo of the Lac de Gras coring site showing the topography of the terrain and turbidity of the water in the littoral zone.

The Horseshoe lake core accumulated with the highest variability of all the lakes. Overall, the accumulation rate is slow, but it is never constant. The core was extracted from a steep-sided sub-basin of the main lake (Figs. 3.1, 5.1). The bathymetry is at a lower resolution than Bridge and Danny's lakes so we cannot see exactly how the

sediments drape over the bedrock. What we can see is that the sub-basin is only connected to the main basin by a shallow (0.5 m deep) passage. The sub-basin therefore would receive little sediment input from snowmelt tributaries. Further, unpublished grain size data from the site shows that the main particle size is sand, whereas most other lakes are silt and clay dominated. There is a nearby esker so presumably the sand would be blown or washed in from there.

5.2 Temporal variability in accumulation rates

Seven of the ten cores that extend past about 7000 cal yr BP show rapid deposition times (~50 yr/cm) at the base of their record and for nearly all these sites this is a much more rapid accumulation rate than average (Fig. 4.2). This rapid accumulation rate is transient and steadily decreases until about 5000 cal yr BP where most lakes with well-constrained age-depth models hit a maximum deposition time – marking the slowest accumulation rate. At all seven sites, the slowest accumulation rate occurs just after a transition from minerogenic-rich sediment at the bottom to organic-rich sediment at the top (Fig. 5.3). This is a common phenomenon in paraglacial environments when sediment availability following glaciation is relatively high as long as there is unstable drift material in fluvial pathways (e.g. Church and Ryder, 1972; Ballantyne, 2002). Sediment availability decreases as it is deposited, but also erosion rates decrease as vegetation is established (Huang et al., 2004). Results from an exponential exhaustion model by Ballantyne (2002) support a decreasing accumulation rate over time as the unstable sediment is deposited. Briner et al. (2010) attribute the transition from minerogenic-rich to organic-rich sediments to be indicative of the catchment for a proglacial lake getting cut off from the

nearby glacier. However, only within the bottom 1 cm of Bridge Lake do we see light grey clay that could be characterized as being deposited in a proglacial setting. Most lakes are characterized by slowest accumulation rates during the period of treeline advance in the region (Kaufman et al., 2004 and references therein), but only the cores with the highest dating resolution (Danny's, Carleton-1B, and Horseshoe lakes) give an indication that accumulation rates begin to increase again during Late Holocene Cooling.

The accumulation rates for the cores from Lac de Gras, Carleton-2012 Lake, and Danny's Lake increase sharply around ~1500 cal yr BP and then decrease around 1300 cal yr BP, creating a small "dip" toward increased accumulation rates (Fig. 4.2). Anderson et al. (2012) also found an increase in mineral accumulation rates at inland and coastal sites from ~1200 to 1000 cal yr BP on southwest Greenland, and attributed this to wind erosion associated with regional cooling and increased aridity. The discrepancy in timing of a few hundred years may be due to the freshwater reservoir correction applied to the Greenland cores. At Carleton Lake, a cooling event between 1690 and 940 cal yr BP was inferred using chironimid proxy data (Upiter et al., *in review*). This period is correlative with the timing of First Millennial Cooling, which has been found in British Columbia (Reyes et al., 2006), Alaska (Hu et al., 2001; Reyes et al., 2006; Clegg et al., 2010), and the Canadian Arctic Archipelago (Thomas et al., 2011). Increased accumulation rates between 1500 and 1300 cal yr BP may correspond to cooling in the central NWT.

5.3 Bayesian age-depth modeling with Bacon

Bayesian age-depth models are designed to be able to handle uncertainties by incorporating prior information (Christen, 1994; Buck et al., 1996; Buck and Millard, 2004; Blaauw and Heegaard, 2012). When the model is fairly straightforward the difference between a Bayesian and non-Bayesian model is minimal, but when the model is more complex (age reversals, shifts in accumulation, hiatuses, etc.) there is more room for disagreement between the models. The difference between the maximum probability age of the Bayesian model and non-Bayesian model for Waite Lake, Danny's Lake, and Horseshoe Lake are presented in Figure 5.4. Waite Lake has the simplest chronology, with only one distinguishable shift in accumulation rate just before 1500 cal yr BP. The difference between the Bayesian and non-Bayesian models is 50 years on average, which is minimal. For Danny's Lake, the difference between the two models is also fairly minimal, about 90 years on average.

The Horseshoe Lake models are 200 years different on average and show the greatest differences (200 – 700 years) where there are shifts in accumulation rate. This is because the smooth spline model constructed with Clam is not as flexible as the Bacon models in areas where accumulation rate changes. The greatest deviances between the Bacon and Clam models for Horseshoe Lake occur at the very bottom of the core (~8000 cal yr BP) and during the Hypsithermal (~5000 cal yr BP). The deviance at the bottom of the core is due to the Bacon model essentially falling apart and at this point, we are not sure why. Moving on to the end of the Hypsithermal and middle of the treeline advance, the Bacon model for Horseshoe Lake suggests that the accumulation rate was so slow that there may have been a hiatus in sediment deposition, whereas the Clam model is much smoother. While the slow accumulation rate could be an artifact of sediment compaction

and dewatering, the rapid accumulation rates preceding this period suggests otherwise; unless the higher minerogenic content at the core bottoms has made the sediment more resistant to compaction.

5.4 Freshwater Reservoir Effect

Reservoir effects in freshwater systems can result from; 1) input of inorganic 'dead' carbon from carbonaceous bedrock or quaternary deposits (Grimm et al., 2009), 2) in-wash of older terrestrial organic mater such as soil and peat (Abbott and Stafford, 1996; Saulnier-Talbot et al., 2009; Blaauw et al., 2011), and 3) the use of aquatic material for dating. In the third case there is a difference been results obtained from aquatic material and terrestrial material due to the lag time between CO_2 in the atmosphere and available CO_2 in the water column. While we could not explicitly determine the FRE for all the sites in this study without paired dating with macrofossils, we could glean information from our results that have helped us better understand potential sources of old carbon in the system.

The central Northwest Territories is underlain by the Slave Craton, which is composed primarily of rocks with a granitic composition and is therefore not likely a source of inorganic 'dead' carbon. In order to assess the proportions of aquatic to terrestrial material in the bulk sediment dates, we examined the $\delta^{13}C$ values that are provided with radiocarbon results (Table 3.1). Aquatic vegetation typically has $\delta^{13}C$ values between -12 and -20‰ and terrestrial or emergent aquatic plant have values around -24 to -30‰ (Oana and Deevey, 1960; Stuiver and Polach, 1977; Aravena et al., 1992). The only lake that consistently plots in the aquatic plant zone is Waite Lake,

which has clear evidence from a twig date and from a modern radiocarbon date near the surface that there is no FRE impacting the radiocarbon dates. Therefore, if there is a reservoir effect associated with the CO_2 exchange between the atmosphere and the aquatic vegetation, it is negligible.

Ruling out these other possibilities, any old carbon in the system would almost certainly have to come from in-wash of older terrestrial organic matter such as soils and peats (Abbott and Stafford, 1996; Saulnier-Talbot et al., 2009; Blaauw et al., 2011). In support of this hypothesis, the majority of outlier dates were older than the model. One possible explanation is that the outliers are derived from older material that was washed into the system, perhaps during a high-energy event such as a storm. Previous studies have shown that the FRE changes over time (e.g. Barnekow et al., 1998; Saulnier-Talbot et al., 2009) with changes in climate and related changes in lake level, vegetation cover, and erosion (e.g. Stuiver, 1975; Geyh et al., 1998; Grimm et al., 2009; Blaauw et al., 2011). Many of the lakes in this study would be sensitive to climate change, as sediment accumulation rates tend to slow down when it is warmer and speed up when it is cooler, most likely reflecting the effectiveness of vegetation cover in preventing erosion. We therefore exercised caution when applying a uniform FRE to our age-depth models.

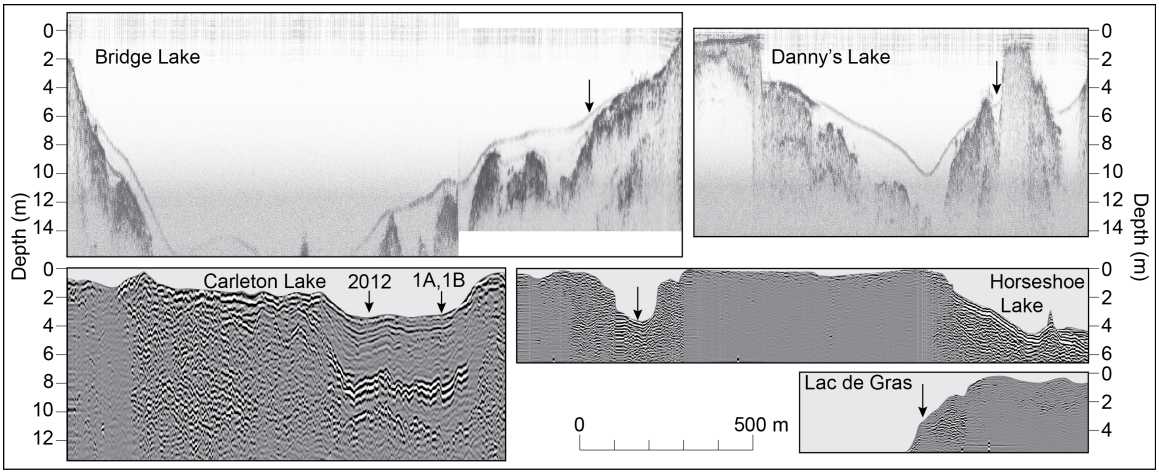

Figure 5.1 Bathymetry profiles from six lakes with arrows shoring coring sites. The coring site for Horseshoe Lake is in a sub-basin that is hydrologically connected to the main basin as is shown in figure 3.

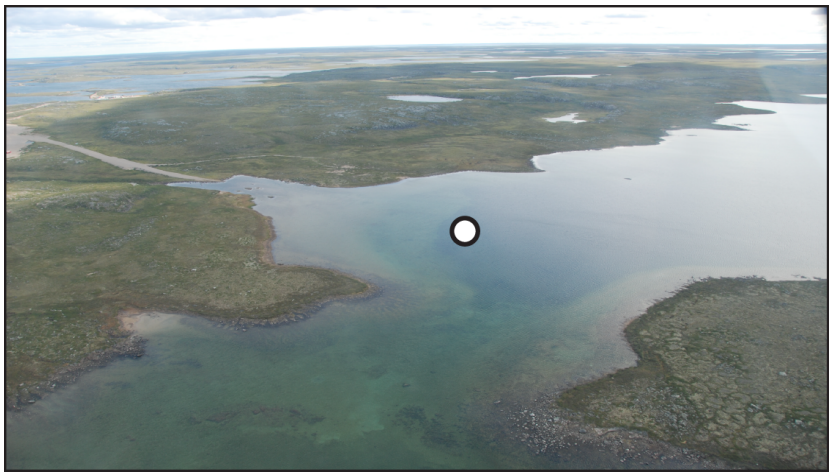

Figure 5.2 Field photo of the Lac de Gras coring site (circle) illustrating the turbulence of the water caused by inlets and the steepness of the slope.

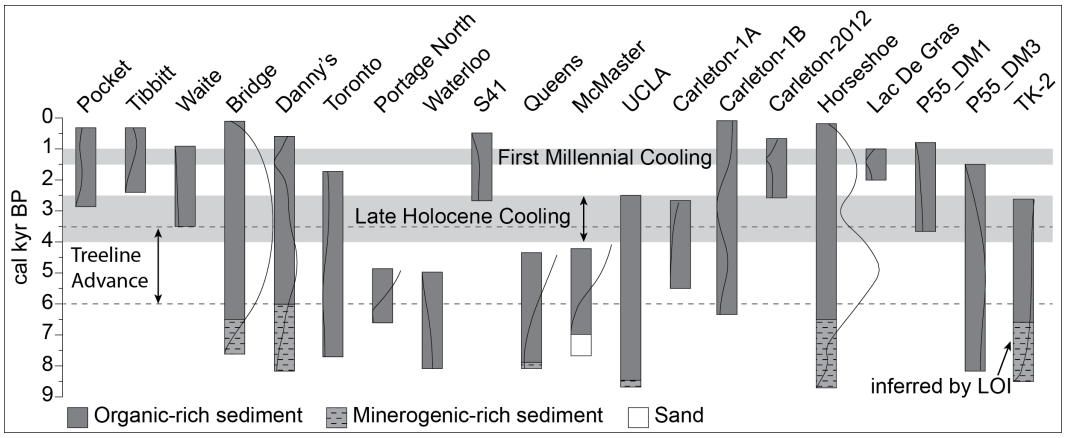

Figure 5.3 Sedimentology of each site, converted to the time scale. The top of each core is defined by the uppermost non-outlying radiocarbon date. Vertical lines are accumulation profiles from Fig. 4.2 and are to be interpreted left to right is faster to slower. Time ranges for the Hypsithermal, treeline advance, and cool period between 4000 and 2500 cal yr BP are from Kaufman et al., (2004) and the references for the First Millennial Cooling can be found in section 5.2.4.

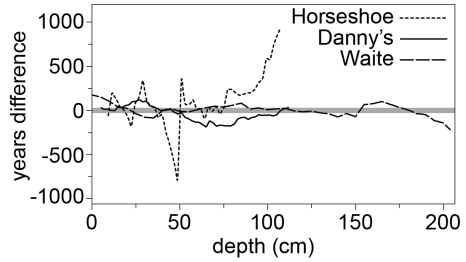

Figure 5.4 Plot showing the difference (in years) versus depth between the models constructed in Clam and Bacon for the Horseshoe, Danny's and Waite Lake cores.

6. Conclusions

Radiocarbon dated lacustrine records from 22 sites at 18 lakes in the central Northwest Territories provide insight into the spatial and temporal changes in lake accumulation rates in the Subarctic region. We conclude that:

1. Rapid accumulation rates (~20 yr/m) occur in lakes with high productivity and high sediment availability. Sites with moderate (~70yr/cm) and slow (>100 yr/cm) accumulation rates exhibit high spatial variability controlled by the dynamics of in-lake bathymetry.

2. Temporal shifts in accumulation rates coincided with centennial to millennial-scale climate change and the waxing and waning of vegetation cover, which is an important mechanism controlling erosion of material into lakes. Post-glacial accumulation rates were rapid, reflecting high sediment availability and low vegetation cover. As vegetation became better established during the treeline advance, we observed a shift from minerogenic-rich to organic-rich sediments and a decrease in accumulation rates, followed by a cool period and increasing accumulation rates between 4000 cal yr BP and 2500 cal yr BP.

3. By elucidating the timing of shifts in accumulation rate in the central NWT, future radiocarbon dating sampling strategies will be better informed about (i) where to add additional radiocarbon dates to better constrain an age-depth model, (ii) how to decide when to stop refining a model, and (iii) better outlier assessment.

7. Future directions / questions

- Tephrochronology at Pocket Lake. Is this the White River Ash? Can we find this chronostratigraphic marker in other cores?
- Develop age-depth models for new cores from the Ice Road project and model their accumulation rates. Test the hypothesis that by understanding when the major regional shifts in lake accumulation occur, we can place radiocarbon dates more strategically.
- Extend study area to encompass more of the Arctic. Perhaps follow the site selection strategy of Kaufman et al. (2004)?
- Constrain the chronology of recent sediments by adding Pb-210, although it can be difficult for Arctic settings. Why is it difficult in Arctic settings?
- Can we use the bathymetry data to choose sites where we can get long cores?
- Isolate pollen to test the freshwater reservoir effect. However, from Blaauw 2010: "since pollen is highly resistant to decay and known to survive long in soils, it may be a significant component of aged carbon from in-washed terrestrial soils or reworked older lake deposits. If so it will contribute to, rather than lessen, the old-carbon age offset (Verschuren, 2003). Kilian et al. (2002) further suggest that allochthonous organic molecules adsorbed to the pollen walls can be another source of contamination". *The sources in this quote are not found in the reference list.
- Is there a hiatus between 4000 and 1000 cal yr BP at Portage Lake North, Waterloo, Queen's, McMaster? Waterloo, Queen's and McMaster were all taken with piston cores and don't have any radiocarbon dates above this horizon. Is it possible that the

tops of these cores were not preserved? They differ from Portage North, which has a radiocarbon date above the potential hiatus.

References

Abbott, M.B., Stafford, T.W., 1996. Radiocarbon geochemistry of modern and ancient Arctic lake systems, Baffin Island, Canada. Quaternary Research 45, 300–311.

Anderson, N.J., Liversidge, A.C., McGowan, S., Jones, M.D., 2012. Lake and catchment response to Holocene environmental change: spatial variability along a climate gradient in southwest Greenland. Journal or Paleolimnology 48, 209–222.

Aravena, R., Warner, B.G., MacDonald, G.M., Hanf, K.I., 1992. Carbon isotope composition of lake sediments in relation to lake productivity and radiocarbon dating. Quaternary Research 37, 333–345.

Ballantyne, C.K., 2002. Paraglacial geomorphology. Quaternary Science Reviews 21, 1935–2017.

Barnekow, L., Possnert, G., Sandgren, P., 1998. AMS ^{14}C chronologies of Holocene lake sediments in the Abisko area, northern Sweden – a comparison between dated bulk sediment and macrofossil samples. GFF 120, 59–67.

Blaauw, M., 2010. Methods and code for 'classical' age-modeling of radiocarbon sequences. Quaternary Geochronology 5, 512–518.

Blaauw, M., Christen, J.A., 2005. Radiocarbon peat chronologies and environmental change. Applied Statistics 54, 805–816.

Blaauw, M., Christen, J.A., 2011. Flexible paleoclimate age-depth models using an autoregressive gamma process. Bayesian Analysis 6, 457–474.

Blaauw, M., van Geel, B., Kristen, I., Plessen, B., Lyaruu, A., Engstrom, D.R., van der Plicht, J., Verschuren, D., 2011. High-resolution ^{14}C dating of a 25,000-year lake-sediment record from equatorial East Africa. Quaternary Science Reviews 30, 3043–3059.

Blaauw, M., Heegaard, E., 2012. Estimation of age-depth relationships. In: Birks, H.J.B., Lotter, A.F., Juggins, S., Smol, P., (Eds.), Tracking Environmental Change Using Lake Sediments. Data Handling and Numerical Techniques. Vol. 5. Springer, Netherlands, pp. 379–413.

Blass, A., Bigler, C., Grosjean, M., Sturm, M., 2007. Decadal-scale autumn temperature reconstruction back to AD 1580 inferred from the varved sediments of Lake Silvaplana (southeastern Swiss Alps). Quaternary Research 68, 184–195.

Bleeker, W., 2002. Archaean tectonics: a review, with illustrations from the Slave craton. Geological Society of London, Special Publications 199, 151–181.

Blockley, S.P.E., Blaauw, M., Bronk Ramsey, C., van der Plicht, J., 2007. Building and testing age models for radiocarbon dates in Lateglacial and Early Holocene sediments. Quaternary Science Reviews 26, 1915–1926.

Briner, J.P., Stewart, H.A.M., Young, N.E., Philipps, W., Losee, S., 2010. Using proglacial-threshold lakes to constrain fluctuations of the Jakobshavn Isbræ ice margin, western Greenland, during the Holocene. Quaternary Science Reviews 29, 3861–3874.

Bronk Ramsey, C., 2009a. Dealing with outliers and offsets in radiocarbon dating. Radiocarbon 51, 1023–1045.

Bronk Ramsey, C., 2009b. Bayesian analysis of radiocarbon dates. Radiocarbon 51, 337–360.

Buck, C.E., Cavanagh, W.G., Litton C.D., 1996. Bayesian approach to interpreting archaeological date. Wiley, Chichester.

Buck, C.E., Millard, A.R. (Eds.), 2004. Tools for constructing chronologies: crossing disciplinary boundaries. Springer-Verlag, London.

Christen, J.A., 1994. Bayesian interpretation of radiocarbon results. Ph.D. thesis, University of Nottingham.

Church, M., Ryder, J.M., 1972. Paraglacial sedimentation: a consideration of fluvial processes conditioned by glaciation. Geological Society of America Bulletin 83, 3059–3072.

Clayton, J.S., Ehrlich, W., Cann, D.B., Day, J.H., Marshall, I.B., 1977. Soils of Canada. Soil Inventory Research Branch, Canada, vol. II. Department of Agriculture, Ottawa. 239 pp.

Clegg, B.F., Clarke, G.H., Chipman, M.L., Chou, M., Walker, I.R., Tinner, W., Hu, F.S., 2010. Six millennia of summer temperature variation based on midge analysis of lake sediments from Alaska. Quaternary Science Reviews 29, 3308–3316.

Cockburn, J.M.H., Lamoureux, S.F., 2008. Inflow and lake controls on short-term mass accumulation and sedimentary particle size in a High Arctic Lake: implications for interpreting varved lacustrine sedimentary records. Journal of Paleolimnology 40, 923–942.

Dyke, A.S., Prest, V.K., 1987. Late Wisconsinan and Holocene history of the Laurentide Ice Sheet. Géographie Physique et Quaternaire 41, 237–263.

Dyke, A.S., Moore, A., Robertson, L., 2003. Deglaciation of North America. Geological Survey of Canada Open File, 1574.

Evans, M., Slaymaker, O., 2004. Spatial and temporal variability of sediment delivery from alpine lake basins, Cathedral Provincial Park, southern British Columbia. Geomorphology 61, 209–224.

Galloway, J.M., Macumber, A.L., Patterson, R.T., Falck, H., Hadlari, T., Madsen, E., 2010. Paleoclimatological assessment of the southern Northwest Territories and implicatons for the long-term viability of the Tibbitt to Contwoyto Winter Road, part 1: core collection. Northwest Territories Geoscience Office, NWT Open Report 2010-002, 21 p.

Geyh, M.A., Schotterer, U., Grosjean, M., 1998. Temporal changes of the ^{14}C reservoir effect in lakes. Radiocarbon 40, 921–931.

Glew, J.R., 1991. Miniature gravity corer for recovering short sediment cores. Journal of Paleolimnology 5, 285–287.

Glew, J.R., Smol, J.P., Last, W.M., 2001. Sediment core collection and extrusion. In: Last, W.M., Smol, J.P. (Eds.), Tracking environmental changes using lake sediments: Volume 1: Basin analysis, coring and chronological techniques. Dordrecht: Kluwer Academic Publishers p 73–105.

Goring, S., Williams, J.W., Blois, J.L., Jackson, S.T., Paciorek, C.J., Booth, R.K., Marlon, J.R., Blaauw, M., Christen, J.A., 2012. Deposition times in the northeastern United States during the Holocene: establishing valid priors for Bayesian age models. Quaternary Science Reviews 48, 54–60.

Grimm, E.C., Maher Jr., L.J., Nelson, D.M., 2009.The magnitude of error in conventional bulk-sediment radiocarbon dates from central North America. Quaternary Research 72, 301–308.

Helmstaedt, H., 2009. Crust-mantle coupling revisited: The Archean Slave craton, NWT, Canada. Lithos 112S, 1055–1068.

Hu, F.S., Ito, E., Brown, T.A., Curry, B.B., Engstrom, D.R., 2001. Pronounced climatic variations in Alaska during the last two millennia. Proceedings of the National Academy of Sciences 98, 10552–10556.

Hua, Q., Barbetti, M., 2004. Review of tropospheric bomb ^{14}C data for carbon cycle modeling and age calibration purposes. Radiocarbon 46, 1273–1298.

Huang, C.C., MacDonald, G., Cwynar, L., 2004. Holocene landscape development and climatic change in the low arctic, Northwest Territories, Canada. Palaeogeography, Palaeoclimatology, Palaeoecology 205, 221–234.

Kaufman, D.S., Ager, T.A., Anderson, N.J., Anderson, P.M., Andrews, J.T., Bartlein, P.J., Brubaker, L.B., Coats, L.L., Cwynar, L.C., Duvall, M.L., Dyke, A.S., Edwards, M.E., Eisner, W.R., Gajewski, K., Geirsdóttir, A., Hu, F.S., Jennings, A.E., Kaplan, M.R., Kerwin, M.W., Lozhkin, A.V., MacDonald, G.M., Miller, G.H., Mock, C.J., Oswald, W.W., Otto-Bliesner, B.L., Porinchu, D.F., Rühland, K., Smol, J.P., Steig, E.J., Wolfe, B.B., 2004. Holocene thermal maximum in the western Arctic (0–180 W). Quaternary Science Reviews 23, 529–560.

Koff, T., Punninga, J.-M., Kangura, M., 2000. Impact of forest disturbance on the pollen influx in lake sediments during the last century. Review of Palaeobotany and Palynology 111, 19–29.

Kulbe, T., Niederreiter Jr., R., 2003. Freeze coring of soft surface sediments at a water depth of several hundred meters. Journal of Paleolimnology 29, 257–263.

Lerbekmo, J.F., 2008. The White River Ash: largest Holocene Plinian tephra. Canadian Journal of Earth Sciences 45, 693–700.

Lotter, A.F., Renberg, I., Hansson, H., Stöckli, R., Sturm, M., 1997. A remote controlled freeze corer for sampling unconsolidated surface sediments. Aquatic Sciences 59, 295–303.

MacDonald, G.M., Edwards, T.W.D., Moser, K.A., Pienitz, R., Smol, J.P., 1993. Rapid response of treeline vegetation and lakes to past climate warming. Nature 361, 243–246.

MacDonald, G.M., Porinchu, D.F., Rolland, N., Kremenetsky, K.V., Kaufman, D.S., 2009. Paleolimnological evidence of the response of the central Canadian treeline zone to radiative forcing and hemispheric patterns of temperature change over the past 2000 years. Journal of Paleolimnology 41, 129–141.

Macumber, A.L., Patterson, R.T., Neville, L.A., Falck, H., 2011. A sledge microtome for high resolution subsampling of freeze cores. Journal of Paleolimnology 45, 307–310.

Macumber, A.L., Neville, L.A., Galloway, J.M., Patterson, R.T., Falck, H., Swindles, G., Crann, C., Clark, I., Gammon, P., Madsen, E., 2012. Paleoclimatological assessment of the Northwest Territories and implications for the long-term viability of the Tibbitt to

Contwoyto Winter Road, part II: March 2010 field season results. Northwest Territories Geoscience Office, NWT Open Report 2011-010, pp. 83.

Marlon, J., Bartlein, P.J., Whitlock, C., 2006. Fire-fuel-climate linkages in the northwestern USA during the Holocene. The Holocene 16, 1059–1071.

Moser, K.A., MacDonald, G.M., 1990. Holocene vegetation change at treeline north of Yellowknife, Northwest Territories, Canada. Quaternary Research 34, 227–239.

Oana, S., Deevey, E.S., 1960. Carbon 13 in lake waters and its possible bearing on paleolimnology. American Journal of Science 258, 253–272.

Padgham, W.A., Fyson, W.K., 1992. The slave province: a distinct Archean craton. Canadian Journal of Earth Science 29, 2072–2086.

Paul, C.A., Rühland, K.M., Smol, J.P., 2010. Diatom-inferred climatic and environmental changes over the last ~9000 years from a low Arctic (Nunavut, Canada) tundra lake. Palaeogeography, Palaeoclimatology, Palaeoecology 291, 205–216.

Pientiz, R., Smol, J.P., MacDonald G.M., 1999. Paleolimnological reconstruction of Holocene climate trends from two boreal treeline lakes, Northwest Territories, Canada. Arctic, Antarctic, and Alpine Research 31, 82–93.

Pyne-O'Donnell, S.D.F., Hughes, P.D.M., Froese, D.G., Jensen, B.J.L., Kuehn, S.C., Mallon, G., Amesbury, M.J., Charman, D.J., Daley, T.J., Loader, N.J., Mauquoy, D., Street-Perrott, F.A., Woodman-Ralph, J., 2012. High-precision ultra-distal Holocene tephrochronology in North America. Quaternary Science Reviews 52, 6–11.

Rampton, V.N., 2000. Large-scale effects of subglacial meltwater flow in the southern Slave Province, Northwest Territories, Canada. Canadian Journal of Earth Science 37, 81–93.

Reimer, P.J., Brown, T.J., Reimer, R.W., 2004. Discussion: reporting and calibration of post-bomb ^{14}C data. Radiocarbon 46, 1299–1304.

Reimer, P.J., Baillie, M.G.L., Bard, E., Bayliss, A., Beck, J.W., Blackwell, P.G., Bronk Ramsey, C., Buck, C.E., Burr, G.S., Edwards, R.L., Friedrich, M., Grootes, P.M., Guilderson, T.P., Hajdas, I., Heaton, T.J., Hogg, A.G., Hughen, K.A., Kaiser, K.F., Kromer, B., McCormac, F.G., Manning, S.W., Reimer, R.W., Richards, D.A., Southon, J.R., Talamo, S., Turney, C.S.M., van der Plicht, J., Weyhenmeyer, C.E., 2009. IntCal09 and Marine09 radiocarbon age calibration curves, 0-50,000 years cal BP. Radiocarbon 51, 1111–1150.

Reyes, A.V., Wiles, G.C., Smith, D.J., Barclay, D.J., Allen, S., Jackson, S., Larocque, S., Laxton, S., Lewis, D., Calkin, P.E., Clague, J.J., 2006. Expansion of alpine glaciers in Pacific North America in the first millennium A.D. Geology 34, 57–60.

Robinson, S.D., 2001. Extending the late Holocene White River Ash distribution, Northwestern Canada. Arctic 54, 157–161.

Rühland, K., Smol, J.P., 2005. Diatom shifts as evidence for recent Subarctic warming in a remote tundra lake, NWT, Canada. Palaeogeoprahy, Palaeoclimatology, Palaeoecology 226, 1–16.

Saulnier-Talbot, E., Pienitz, R., Stafford Jr., T.W., 2009. Establishing Holocene sediment core chronologies for northern Ungava lakes, Canada, using humic acids (AMS ^{14}C) and ^{210}Pb. Quaternary Geochronology 4, 278–287.

Schiefer, E., 2006. Contemporary sedimentation rates and depositional structures in a montane lake basin, southern Coast Mountains, British Columbia, Canada. Earth Surface Processes and Landforms 31, 1311–1324.

Smith, D.G., 1994. Glacial Lake McConnell: paleogeography, age, duration, and associated river deltas, Mackenzie River Basin, Western Canada. Quaternary Science Reviews 13, 829–843.

Stuiver, M., 1975. Climate versus changes in ^{13}C content of the organic components of lake sediments during the late Quaternary. Quaternary Research 5, 251–262.

Stuiver, M., Polach, H.A., 1977. Discussion: reporting of 14C data. Radiocarbon 19, 355–363.

Stuiver, M., Reimer, P.J., 1993. Extended ^{14}C database and revised Calib 3.0 ^{14}C age calibration program. Radiocarbon 35, 215–230.

Thomas, E.K., Briner, J.P., Axford, Y., Francis, D.R., Miller, G.H., Walker, I.R., 2011. A 2000-yr-long multi-proxy lacustrine record from central Baffin Island, Arctic Canada reveals first millennium AD cold period. Quaternary Research 75, 491–500.

Upiter, L.M., Vermaire, J.C., Patterson, R.T., Crann, C., Galloway, J.M., Macumber, A.L., Neville, L.A., Swindles, G.T., Falck, H., Roe, H.M., Pisaric, M.F.J., *in review*. A mid- to late Holocene chironomid-inferred temperature reconstruction for the central Northwest Territories, Canada. Journal of Paleolimnology.

Webb, R.S., Webb, T., 1988. Rates of sediment accumulation in pollen cores from small lakes and mires of eastern North America. Quaternary Research 30, 284–297.

Wedel, J.H., Smart, A., Squires, P., 1990. An overview study of the Yellowknife river basin, N.W.T. N.W.T. programs: inland waters directorate conservation and protection. Western and Northern Region, Environment Canada, Ottawa.

Wolfe, B.B., Edwards, T.W.D., Aravena, R., MacDonald, G.M., 1996. Rapid Holocene hydrologic change along boreal tree-line revealed by $\delta^{13}C$ and $\delta^{18}O$ in organic lake sediments, Northwest Territories, Canada. Journal of Paleolimnology 15, 171–181.

Wright Jr., R.G., Mann, D.H., Glaser, P.H., 1984. Piston cores for peat and lake sediments. Ecology 65, 657–659.